



Millimeter-Wave Radar Field Measurements and Inversion of Cloud Parameters for the 1999 Mt. Washington Icing Sensors Project

Andrew L. Pazmany
Quadrant Engineering, Inc., Amherst, Massachusetts

The NASA STI Program Office . . . in Profile

Since its founding, NASA has been dedicated to the advancement of aeronautics and space science. The NASA Scientific and Technical Information (STI) Program Office plays a key part in helping NASA maintain this important role.

The NASA STI Program Office is operated by Langley Research Center, the Lead Center for NASA's scientific and technical information. The NASA STI Program Office provides access to the NASA STI Database, the largest collection of aeronautical and space science STI in the world. The Program Office is also NASA's institutional mechanism for disseminating the results of its research and development activities. These results are published by NASA in the NASA STI Report Series, which includes the following report types:

- **TECHNICAL PUBLICATION.** Reports of completed research or a major significant phase of research that present the results of NASA programs and include extensive data or theoretical analysis. Includes compilations of significant scientific and technical data and information deemed to be of continuing reference value. NASA's counterpart of peer-reviewed formal professional papers but has less stringent limitations on manuscript length and extent of graphic presentations.
- **TECHNICAL MEMORANDUM.** Scientific and technical findings that are preliminary or of specialized interest, e.g., quick release reports, working papers, and bibliographies that contain minimal annotation. Does not contain extensive analysis.
- **CONTRACTOR REPORT.** Scientific and technical findings by NASA-sponsored contractors and grantees.

- **CONFERENCE PUBLICATION.** Collected papers from scientific and technical conferences, symposia, seminars, or other meetings sponsored or cosponsored by NASA.
- **SPECIAL PUBLICATION.** Scientific, technical, or historical information from NASA programs, projects, and missions, often concerned with subjects having substantial public interest.
- **TECHNICAL TRANSLATION.** English-language translations of foreign scientific and technical material pertinent to NASA's mission.

Specialized services that complement the STI Program Office's diverse offerings include creating custom thesauri, building customized data bases, organizing and publishing research results . . . even providing videos.

For more information about the NASA STI Program Office, see the following:

- Access the NASA STI Program Home Page at <http://www.sti.nasa.gov>
- E-mail your question via the Internet to help@sti.nasa.gov
- Fax your question to the NASA Access Help Desk at 301-621-0134
- Telephone the NASA Access Help Desk at 301-621-0390
- Write to:
NASA Access Help Desk
NASA Center for Aerospace Information
7121 Standard Drive
Hanover, MD 21076



Millimeter-Wave Radar Field Measurements and Inversion of Cloud Parameters for the 1999 Mt. Washington Icing Sensors Project

Andrew L. Pazmany
Quadrant Engineering, Inc., Amherst, Massachusetts

Prepared under Contract C-75630-J

National Aeronautics and
Space Administration

Glenn Research Center

Available from

NASA Center for Aerospace Information
7121 Standard Drive
Hanover, MD 21076

National Technical Information Service
5285 Port Royal Road
Springfield, VA 22100

Available electronically at <http://gltrs.grc.nasa.gov/GLTRS>

I. DEFINITION OF VARIABLES.....	1
II. GLOSSARY	2
1. INTRODUCTION.....	4
2. EXPERIMENT CONFIGURATION.....	4
2.1 RADAR SYSTEM DESCRIPTION	7
2.1.1 NOAA-ETL X-band Atmospheric Radar	7
2.1.2 UMass 33/95 GHz CPRS System.....	7
3. RADAR DATA ARCHIVE.....	8
4. BACKGROUND ON THE MULTI-FREQUENCY RADAR INVERSION ALGORITHM	9
5. RESULTS OF NEURAL NETWORK INVERSIONS ON SELECTED DATA SETS.....	11
6. COMPARISON OF RADAR-DERIVED LWC WITH IN-SITU DATA FROM ATEK PROBE...12	
REFERENCES	14
APPENDIX A: LIQUID WATER CONTENT, MVD, AND MZD EXTRACTED FROM MULTIFREQUENCY REFLECTIVITY PROFILES.	15

I. Definition of Variables

α	shape parameter for gamma distribution; larger values of α yield a narrower distribution.
c	speed of light ($2.997e8$ m/s).
C	correlation factor ($0 < C < 1$) to determine overlap between range gates.
D	particle diameter (m).
dBZ	Radar Reflectivity Factor; proportional to D^6 .
$dBZe$	Radar Equivalent Reflectivity Factor; radar measured dBZ assuming Rayleigh scatterers (used with millimeter wave radars when particles are often Mie).
E_{LWC}	RMS error of the neural net estimated LWC (g/m^3).
E_{MVD}	relative RMS error of the neural net estimated MVD (%).
E_{MZD}	relative RMS error of the neural net estimated MZD (%).
f	frequency (Hertz).
γ	shape parameter for gamma distribution. Larger γ values yield narrower distributions.
k_w	extinction due to liquid water (dB/km).
K	complex quantity related to the index of refraction of water or ice.
λ	electromagnetic wavelength (m).
L_a	atmospheric loss (dB/km).
LWC	liquid water content ($g \cdot m^{-3}$).
MD	Mean Diameter (μm).
MVD	Mean Volume Diameter (μm).
MZD	Mean Z Diameter (μm).
LWC_{NN}	Neural Net Estimated Liquid Water Content ($g \cdot m^{-3}$).
MVD_{NN}	Neural Net Estimated Mean Volume Diameter (μm).
MZD_{NN}	Neural Net Estimated Mean Z Diameter (μm).
η	volume backscattering coefficient ($m^2 \cdot m^{-3}$).
N	index of refraction.
N_i	number of input nodes in neural network.
N_r	number of range gates sampled by neural network.
N_f	number of frequencies sampled by neural network.
N_p	number of output parameters of the neural network.
N_o	number of output nodes in neural network.
N_{ave}	number of radar samples averaged (power average).
N_0	number density parameter for the Marshall-Palmer distribution.
ϕ	general angular variable.
ϕ_{az}	scan range in azimuth (radians).
ϕ_{el}	scan range in elevation (radians).
$p(r)$	drop size distribution (number of drops per cubic meter per meter diameter).
P_t	radar transmit power (W).
P_{min}	minimum detectable received power (W).
r_c	mode radius (radius corresponding to the peak value of the drop size distribution).
r	particle radius (μm).
R	radar range (m).
τ	pulse length (s).
Z	cloud reflectivity ($mm^6 \cdot m^{-3}$). Z_{vv} is the copolarized reflectivity for transmission and reception of vertical polarization; Z_{hh} is the copolarized reflectivity for transmission and

reception of horizontal polarization; Z_{vh} is the cross-polarized reflectivity, for transmission of horizontal and reception of vertical polarization.

II. Glossary

- **Drop-size Distribution** - The measured or modeled distribution of drop diameters for clouds or rain. Units are number of drops per meter per cubic meter or m^{-4} .
- **Ka-band** – The electromagnetic frequency interval between 28 and 40 *GHz*.
- **Liquid Water Content (LWC)** - The water content, in grams per cubic meter, of the liquid portion of the cloud or precipitation.
- **Mean Volume Diameter (MVD)** - Particle diameter corresponding to the mean of the volume distribution. Volume distribution is computed from the given drop size (diameter) distribution. Note that median volume diameter (denoted *MeVD* in this report) is a much more commonly used icing variable.
- **Median Volume Diameter (MeVD)** - Particle diameter corresponding to the median of volume distribution. This is usually denoted by *MVD* in the icing literature.
- **Mean Z Diameter (MZD)** - Particle diameter corresponding to mean cloud reflectivity.
- **Mie Scattering** - Mie scattering refers to the complete solution for electromagnetic scattering from dielectric spheres as computed by G. Mie in 1908. This relatively complicated formulation is required when the particle size is within an order of magnitude of the electromagnetic wavelength. Approximate formulas are often used in the optical limit ($d \gg \lambda$) and Rayleigh limit ($d \ll \lambda$) to simplify calculations.
- **Multiparameter Radar** - Radar system capable of measuring a variety of parameters at one or more frequencies. For a meteorological radar, these parameters include cloud reflectivity, Doppler spectrum of the scattered signal (or its moments), and four additional polarimetric parameters, including linear depolarization ratio *LDR*, differential reflectivity Z_{dr} , and the magnitude and phase of the copolarized correlation coefficient, ρ_{hv} .
- **Neural Network** - A software algorithm used to determine output parameters based on a network of interconnected summing nodes with non-linear response to the input. The neural network was originally developed to imitate the function of interconnected brain neurons. The basic building block of neural networks are non-linear summing nodes that are coupled to other nodes through connections with variable weighting factors. These weighting factors, along with the transfer function of the summing nodes, are adjusted to minimize estimation errors by using a set of known input and output vectors.
- **PPI (Plan Position Indicator)** – A range versus azimuth angle display of radar parameters in polar coordinates. During a PPI scan, the antenna beam is scanned in azimuth at a fixed elevation angle.
- **RHI (Range Height Indicator)** – A range versus elevation angle display of radar parameters in polar coordinates. During an RHI scan the radar beam is scanned in elevation at a constant azimuth angle.

- **Rayleigh Scattering** - Simplified scattering regime for particles much smaller than the electromagnetic wavelength. For larger particles, on the order of the radar wavelength, the complete Mie solution must be computed. Scattering from particles much larger than the electromagnetic wavelength can be approximated using optical limit formulas.
- **X-band** – The electromagnetic frequency interval between 8 and 12 GHz.
- **W-band** – The electromagnetic frequency interval between 75 and 100 GHz.
- **Reflectivity, Z** - Frequency-independent parameter equal to the sixth moment of drop-size distribution. Reflectivity is proportional to backscattered power. The sixth moment arises from the fact that the radar cross-section of a small particle ($d \ll \lambda$) is proportional to the sixth power of particle diameter. Reflectivity is typically expressed on a decibel scale, as dBZ which equals $10 \log_{10}(Z)$.

1. Introduction.

The Mount Washington Icing Sensors Project (MWISP) was a multi-investigator experiment with participants from Quadrant Engineering, NOAA Environmental Technology Laboratory (NOAA/ETL), the Microwave Remote Sensing Laboratory (MIRSL) of the University of Massachusetts (UMass) and others. Radar systems from UMass and NOAA/ETL were used to measure X-, Ka- and W-band backscatter data from the base of Mt. Washington, while simultaneous in-situ particle measurements were made from aircraft and from the observatory at the summit. This report presents range and time profiles of liquid water content and particle size parameters derived from range profiles of radar reflectivity as measured at X-band, Ka-band and W-band (9.3, 33.1 and 94.9 GHz) using an artificial neural network inversion algorithm.

In this report, we provide a brief description of the experiment configuration, radar systems and a review of the artificial neural network used to extract cloud parameters from the radar data. Time histories of liquid water content (*LWC*), mean volume diameter (*MVD*) and mean Z diameter (*MZD*) are plotted at 300 *m* range intervals for slant ranges between 1.1 and 4 *km*. Appendix A provides details on the extraction of radar reflectivity from measured radar power, and Appendix B provides summary logs of the weather conditions for each day in which we processed data.

2. Experiment configuration.

A diagram of the experiment configuration is shown in Figure 1. A variety of remote sensing instruments were set up at the cog rail base, summarized in Table 1. In-situ probes are summarized in Table 2. Figure 1, Tables 1 and 2, and other specific data included in this section were excerpted from two MWISP web sites: <http://www.faa.gov/aua/awr/mwisp> and <http://www.rap.ucar.edu/projects/mwisp> .

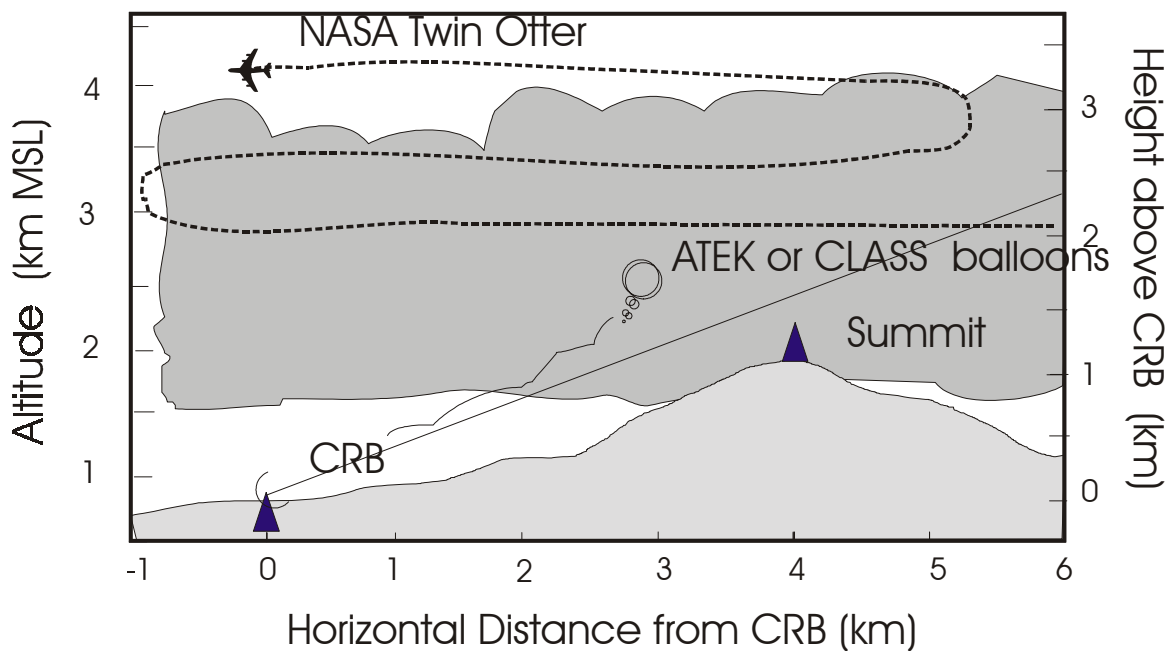


Figure 1: MWISP layout. Profile is along an approximate west to east line connecting the Cog Railway Base (CRB) and the Mt. Washington Observatory at the summit (this figure was excerpted from the MWISP science plan).

MWISP SITE COORDINATES

(Based on hand-held GPS and topo map)

Mount Washington Observatory (MWO):

Latitude = 44 deg., 16 min., 15 sec N
 Longitude = 71 deg., 18 min., 14 sec W
 Altitude = 6267 ft = 1910 m MSL
 Declination = -16.0 deg.

Cog Rail Base (CRB) remote sensors:

Latitude = 44 deg., 16 min., 10 sec. N
 Longitude = 71 deg., 21 min., 11 sec. W
 Altitude = 2660 ft = 811 m MSL
 Declination = -16.6° (magnetic N is 16.6 degrees west of true N)

CRB to MWO:

horiz. distance = 3.9 km
 slant range = 4.1 km
 azimuth = 87 deg. from true north
 elevation = 15.9 deg.

Table 1: MWISP Remote Sensors

What	Location	Whose	Funded By
NOAA K Radar	CRB	NOAA ETL	FAA (IFIPDT)
NOAA X Radar	CRB	NOAA ETL	FAA (IFIPDT)
UMass Ka-band	CRB	UMass	NASA
UMass W-band	CRB	UMass	NASA
Polarimetric Scanning Radiometer (PSR)	Summit	NOAA ETL	NASA
Lidar	CRB	DREV	NASA
Dual-channel microwave radiometer (Radiometrics)	CRB	WJHTC	MWO (from FAA)
Ceilometer	CRB	WJHTC	MWO (from FAA)
Dual-channel tippable microwave radiometer	CRB	NOAA ETL	FAA (IFIPDT)

Table 2: MWISP In Situ Sensors

What	Location	Who	Funded By
CLASS soundings	Variable (from mobile unit)	NCAR	FAA (IFIPDT)
ATEK soundings	CRB/Bretton Woods	ATEK Inc.	CRREL, FAA (IFIPDT)
Snowgages	Heli pad near summit, CRB	NCAR	FAA (WWPDT, IFIPDT)
Particle Measuring Systems, Inc. Probes (FSSP, 2D-G/12.5 μm and 2D-G 100 μm)	Summit	CRREL	FAA (IFIPDT), CRREL
Cloud Scope	Summit	Desert Research Institute/MWO	MWO
Cloud Particle Imager (CPI)	Summit	Stratton Park Engineering, Inc. (SPEC)	NASA, FAA (IFIPDT)
NASA Twin Otter Aircraft	Aloft	NASA Lewis Research Center	NASA

2.1 Radar System Description

2.1.1 NOAA-ETL X-band Atmospheric Radar

An X-band (9.34 *GHz*) radar provided by NOAA/ETL, termed NOAA/D shown in Figure 2-a, is a high power, dual-polarization mobile radar. The radar transmits 25-*kW* of peak power in a 0.9-*degree* circular beam using a 10-*ft* (3.05-m)diameter parabolic dish. Radial velocity, reflectivity, and depolarization are measured at 328 range gates using PPI, RHI, or fixed-beam scans. Range resolution was set to 75 *m* for the MWISP experiment. Groups of four range gates were averaged together to match the resolution of the neural network training data set (300 *m*). Sensitivity is approximately 10 *dBZ* at 25-*km* range.

Summary of NOAA/D X-band radar operating parameters for MWISP:

Frequency:	X-band (9.3 <i>GHz</i>)
Range resolution:	75 <i>m</i> (four range gates averaged).
Azimuth resolution at 2 <i>km</i> :	31 <i>m</i> .
Number time samples averaged per gate:	256
Polarization:	Horizontal linear



Figure 2-a. The NOAA/D, NOAA-ETL's X-band atmospheric radar .

2.1.2 Umass 33/95 GHz CPRS System

The Cloud Profiling Radar System (CPRS) uses a dual-frequency, dual polarization 1.0 *m* diameter lens antenna to produce co-axial beams at 33 and 95 *GHz*. The radar generates a peak power of 100 *kW* at 33 *GHz* and 1.2 *kW* at 95 *GHz*, providing sufficient sensitivity to study non-precipitating clouds to ranges of 15 *km* or greater. In order to maximize the sensitivity of the radar, only vertical polarized pulses were used for the measurements. Each measured data point was calculated by averaging the scattered power from 200

transmit pulses. The pulses were transmitted in groups of four, with pulses spaced $150\ \mu\text{s}$ within the groups and the groups were spaced at $1\ \text{ms}$. We estimate that the decorrelation time of a typical atmospheric target (velocity spectral width of $1.5\ \text{m/s}$) is approximately $3\ \text{ms}$ at $33\ \text{GHz}$ and $1\ \text{ms}$ at $95\ \text{GHz}$. As a result, an equivalent of about 16 independent samples at Ka-band and 50 independent samples at W-band were averaged for each recorded data point for the reduction of fading but all 200 pulses helped improve signal to thermal noise ratio.

Summary of CPRS operating parameters for MWISP (Ka-band):

Frequency:	$33.12\ \text{GHz}$
Range Resolution:	$30\ \text{m}$ (ten range gates averaged)
Azimuth resolution at $2\ \text{km}$:	$22\ \text{m}$
Number of time samples averaged per gate:	200 (16 independent)
Polarization:	Vertical linear

Summary of CPRS operating parameters at W-band:

Frequency:	$94.92\ \text{GHz}$
Range Resolution:	$75\ \text{m}$ (four range gates averaged)
Azimuth resolution at $2\ \text{km}$ slant range:	$8\ \text{m}$
Number of time samples averaged per gate:	200 (50 independent)
Polarization:	Vertical linear



Figure 2-b. The UMass 33/95 GHz Cloud Profiling Radar System at the MWISP base camp.

3. Radar data archive.

The UMass Ka- and W-band radar system collected data from April 4 to April 26, 1999. The measured data, which was converted to Net CDF format, along with quick look images of various radar parameters, can be accessed via the Internet at <http://abyss.ecs.umass.edu/CPRS>. X-band data from NOAA/D was received directly from NOAA on tape.

4. Background on the Multi-frequency Radar Inversion Algorithm

In 1998 Quadrant Engineering Inc. completed a study to assess remote sensing techniques for the detection and mapping of aircraft icing potential. The problem was constrained to a forward looking volume imaging remote sensing system capable of measuring cloud and precipitation parameters, such as Liquid Water Content (*LWC*), and drop size at about 1 km range resolution out to 20-30 km. The measurement concept for an in-flight sensor system is illustrated in Figure 3.

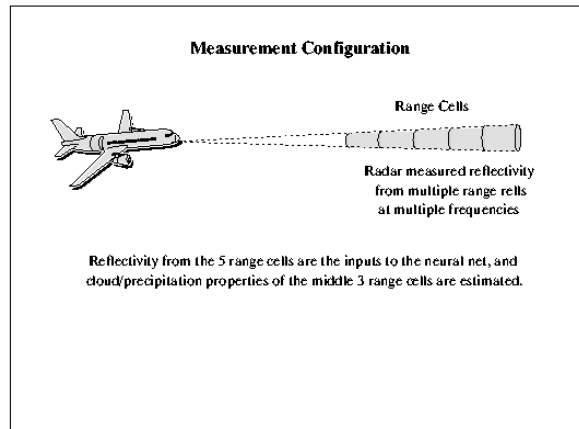


Figure 3. Measurement concept of an in-flight icing detection remote sensing system.

After analyzing a variety of active and passive remote sensor combinations, multi-frequency radar was identified as the most promising technology for the problem. The technique involves the simultaneous processing of 10, 35 and 95 GHz radar reflectivity profiles with an artificial neural network to estimate *LWC* and drop size in clouds and precipitation. Computer simulations indicated that *LWC*, and drop size measured as Medium Volume Diameter (*MVD*), and Mean Z Diameter (*MZD*), can be estimated with reasonable accuracy, even in the presence of significant (1 dB) estimation errors [1].

Multi-frequency radar has an excellent potential for probing cloud particle parameters due to the combination of moderate attenuation and adequate scattering cross-section. In the original 1998 study, Quadrant Engineering Inc. formulated a working hypothesis that cloud parameters could be extracted by measuring backscatter at a combination of attenuating and non-attenuating frequencies. Since scattering is a complex nonlinear function of particle size and frequency, it is impractical to consider an analytical solution to the inverse problem of computing particle size and liquid water content based on measured backscattered power at multiple frequencies. Quadrant therefore focused its efforts on an approximate numerical solution to the inversion, specifically, a neural network. The network was trained by simulating thousands of test cases of radar scattering from assumed particle size distributions.

The inverse problem of extracting cloud parameters from the measured range profiles of backscattered power is a good example of a problem without well defined rules for estimation. The forward problem is straightforward: for a given drop-size distribution, reflectivity and attenuation can easily be calculated using Mie scattering formulas [2]. Also, cloud and precipitation properties, such as liquid water content or rain rate, can be directly calculated from drop-size distribution. Solving the inverse problem, that is, calculating cloud parameters from measured reflectivity profiles, is very difficult, due to the non-linearity of the forward problem. Neural nets are ideal for solving problems where the forward problem is well characterized but the inverse is non-linear and complicated. The procedure of this computer simulation is summarized in Figure 4. The simulation first generated a large set of artificial cloud and precipitation conditions, specified in terms of profiles of drop size distributions. From these drop size distributions, the computer algorithm then calculated the corresponding radar observed reflectivity profiles at each operating frequency as well as LWC and drop size in each volume cell. Gaussian distributed random variables were added to the reflectivity profiles to simulate the effect of noise in the data, and this set of multi-frequency radar reflectivity (inputs) and cloud and precipitation parameter profiles (outputs) were then used to train an artificial neural network. A statistically independent, but still simulated, data set was used to evaluate the ability of the neural net to estimate LWC and drop size from the radar data.

In an attempt to train the neural network for potential ice particles in the sample volumes, half of the training data set range cells were biased with a uniformly distributed ice reflectivity between 0 and 3 dB relative to the reflectivity of the liquid particles. It was assumed that the ice particles did not contribute to the attenuation of the cell. There were no other preparations made to the neural network algorithm or tests performed on the measured data to account for the presence or absence of ice particle. It is therefore expected that ice particles introduced additional errors in all the estimated cloud and precipitation parameters. The presence of significant ice particles, beyond the 3 dB reflectivity bias considered in the training data set, would lead to an overestimation of the retrieved liquid drop size parameters, because the algorithm would account for the additional reflectivity by increasing the liquid drop size parameter. The retrieved LWC can also be affected, because ice crystals are often Mie scatterers at W-band (and sometimes at Ka-band), so size variations in range will appear as differential reflectivity gradients either lowering or increasing the neural net estimated LWC . The three frequency (X, Ka and W) network estimated LWC will be the least affected, however, as the third frequency will help estimate the Mie modulation.

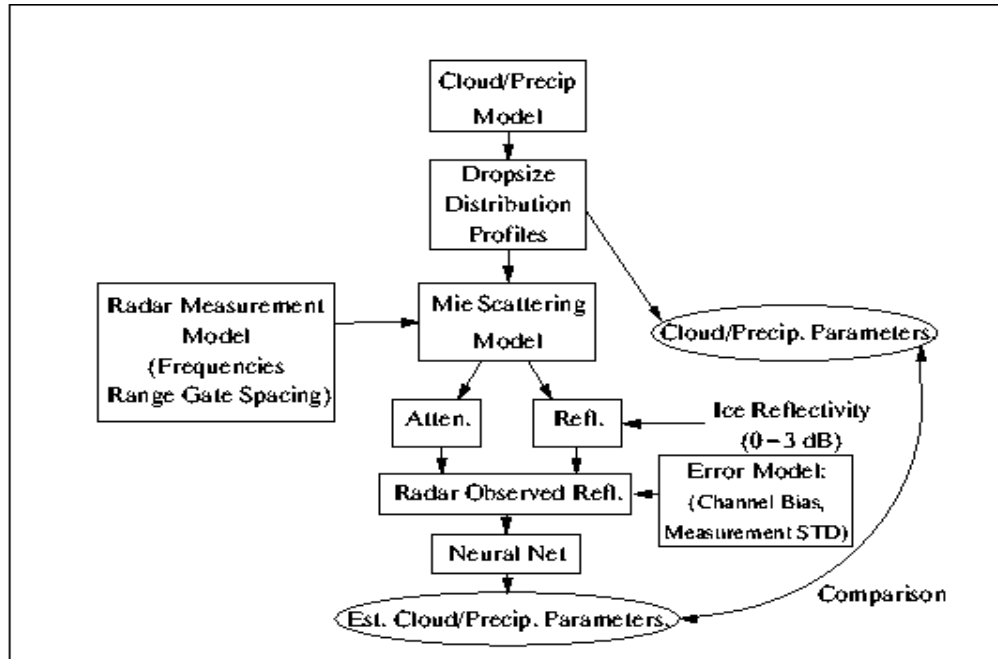


Figure 4. Evaluation of the multi-frequency radar technique for the measurement of cloud and precipitation parameters with simulated data.

5. Results of neural network inversions on selected data sets.

In order to test the accuracy of the neural network algorithm, we processed seventeen data sets, each consisting of twelve minutes of data gathered at X, Ka and W-band. These data sets were interpolated to match up the sampling intervals in range and time. In addition to the averaging described in section 2.1, a sliding boxcar window was used to average over 20 range profiles (20 seconds total averaging) before processing by the neural network.

Data were processed from April 14, 15, 17, 20 and 26, 1999. Figure 5 illustrates the slant ranges where the neural net estimated time series of liquid water content (LWC), mean volume diameter (MVD) and mean Z diameter (MZD). Figures A1-A17, found in Appendix A, show similar plots for all of the processed data. The X-band radar reflectivity image and the corresponding neural net retrieved LWC , MVD , and MZD , shown in Figure 5, were collected through a melting layer at a 19 deg slant angle. Although, in situ data was not available for comparison, the melting layer qualitatively verified the results of the algorithm. The top of the bright band (melting band) is around

1.3 km slant range - just below the second of four range cells of retrieved precipitation parameters. Above the melting band, LWC is just above 0.2 gm^{-3} and the particle size parameters are around 1.5 mm , indicating large ice crystals with some super-cooled liquid. The lowest range cell, centered at the bottom of the bright band, however, shows a much higher LWC , up to 0.8 gm^{-3} , and distinctly smaller drops ranging from 0.5 to 1 mm , confirming the melting of the larger ice crystals into smaller liquid hydrometeors.

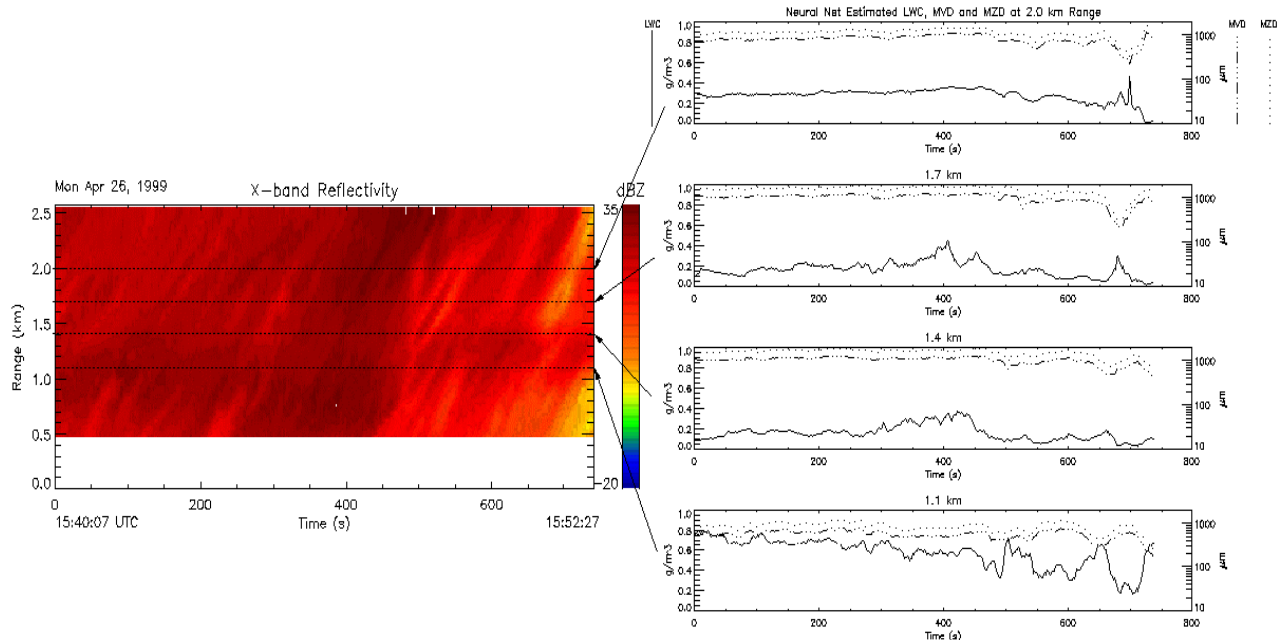


Figure 5. X-band reflectivity image of a melting layer, measured on April 26, 1999, and the corresponding neural net estimated time series of liquid water content (LWC), mean volume diameter (MVD) and mean Z diameter (MZD) at slant ranges 1.1 km , 1.4 km , 1.7 km and 2 km .

6. Comparison of radar-derived LWC with in-situ data from ATEK probe.

A comparison of LWC derived from three frequency radar data shows good agreement with in-situ measurements of liquid water content as derived from balloon soundings of LWC made with the ATEK probe. Figure 6 shows altitude profiles of LWC as measured by the ATEK probe at two times that coincide with radar measurements, April 14 at 19:07 UTC, and April 17 at 17:19 UTC. The asterisks show the average LWC , as derived by the neural network. These points were computed by taking 12-minute averages of the neural network derived LWC at each altitude. The complete time histories of the neural network output used to compute these points can be found in Appendix A, figures A.6 and A.13. Note that slant range in A.6 and A.13 was converted to altitude using the formula in Appendix A.

Figure 6 shows good agreement between the in situ derived liquid water content and the water content measured by the neural network. On April 14, the two measurements show agreement both in the altitude distribution (within 100 m) and peak value (within 20 percent). The agreement in height is not as good on April 17, although the trend towards higher water contents at higher altitudes is the same for both measurement techniques.

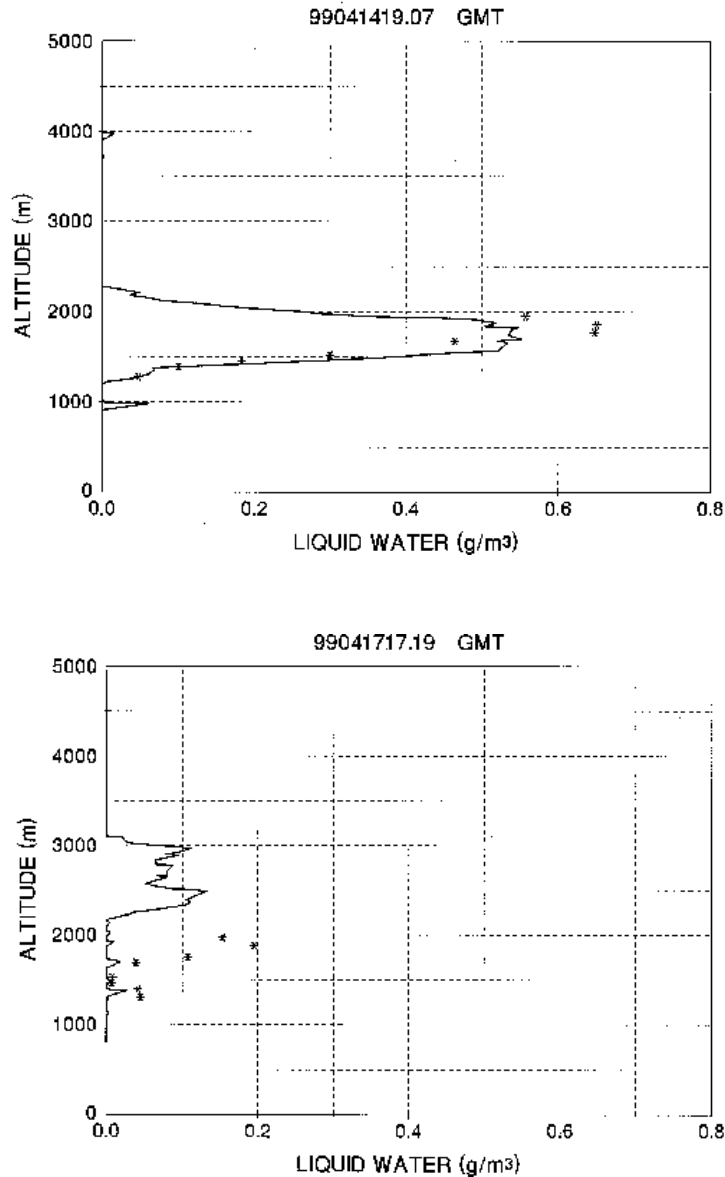


Figure 6. Neural net estimated Liquid water content (*LWC*) averaged over the 12+ minute observation period (*) overlaid on the *LWC* measured in-situ with the ATEK probe (solid line) on April 14, 19:07 UTC (top, compare to Figure A.6), and April 17, 17:19 UTC (bottom, compare to Figure A.13). The cog railway is located at an altitude of 811 m, while the summit of Mt. Washington is located at an altitude of 1910 m.

REFERENCES

- [1] Quadrant Engineering, "Evaluation of Technologies for the Design of a Prototype In-Flight Remote Aircraft Icing Potential Detection System," Final R&D Report, Contract No. DACA39-97-M-1476, 85 pp., 1998.
- [2] Ulaby, F. T., R. K. Moore, A. K. Fung, "Microwave Remote Sensing", Volume II, *Artech House*, 1982, pp. 1064 .
- [3] Doviak, R. J., D. S. Zrnic, "Doppler Radar and Weather Observations", *Academic Press*, 1984, pp. 562.

Appendix A: LWC, MVD, and MZD extracted from multifrequency reflectivity profiles.

Figures A1-A17 provide time histories of *LWC*, *MVD* and *MZD* as derived by the artificial neural network. Table A.1 summarizes the dates, time interval and slant ranges for which the neural network provided cloud parameters for each figure. Slant range, R_s , can be converted to altitude by the following formula: $\text{Altitude} = 0.3256R_s + 811 \text{ m}$.

Table A.1 Table of Figures, Appendix A.

<i>Figure</i>	<i>Date</i>	<i>Time (UTC)</i>	<i>Slant ranges</i>
A.1	April 14, 1999	15:10-15:23	1.1-2.0 km
A.2	April 14, 1999	15:23-15:35	1.1-2.0 km
A.3	April 14, 1999	17:00-17:12	1.1-2.0 km
A.4	April 14, 1999	17:30-17:42	1.1-2.0 km
A.5	April 14, 1999	17:38-17:49	1.1-2.0 km
A.6a/b	April 14, 1999	19:06-19:18	1.4-3.5 km
A.7	April 14, 1999	19:16-19:28	1.1-2.0 km
A.8	April 14, 1999	19:30-19:42	1.1-2.0 km
A.9	April 14, 1999	19:42-19:55	1.1-2.0 km
A.10	April 15, 1999	18:34-18:47	1.1-2.0 km
A.11	April 17, 1999	13:15-13:27	1.1-2.0 km
A.12	April 17, 1999	13:30-13:43	1.1-2.0 km
A.13a/b	April 17, 1999	17:07-17:19	1.4-3.5 km
A.14	April 17, 1999	17:14-17:28	1.1-2.0 km
A.15	April 20, 1999	18:30-18:42	1.1-2.0 km
A.16a/b	April 20, 1999	18:42-18:55	1.4-3.5 km
A.17	April 26, 1999	15:40-15:52	1.1-2.0 km

April 14, 1999

Weather log entry:

Date: 14 april

Time: 2135z

Entry by: m politovich

Entry:

Not a great day but not too bad either.

Same clouds we have been seeing do a circle dance around that low over Labrador. Clouds were thick and thin, 1, 2, 3 layers. Some waves downwind (south/east) of the mountains. Liquid up and down all day. Did not look good enough for the plane to sample so we called them down, and then lo and behold the cloud thickened and the liquid came back. C'est la vie. Still, however, it was no great shakes for an airplane to sample. Lots of dendrites and plates in the cloud, snow showers at the cog base, snow and rime at the summit. Instruments worked well for the most part and we did get a good study in.

The neural net retrieved cloud parameters reflect the snow and variable LWC . The estimated liquid drop equivalent sizes were consistently high, ranging from 100 to 600 micron, while LWC was near zero in the first few files (Figures A.1 and 2) taken after 15:00 UTC. Later files (Figures A.3-5) show sporadic concentrations of higher LWC , up to 0.3 gm^{-3} until the clouds thickened after 19:00 UTC, producing longer range radar data and retrieval out to 3.5 km (Figure A.6a and A.6b). At these upper layers much higher concentrations of liquid was found, up to 0.7 gm^{-3} . This liquid layer was confirmed by the ATEK probe measured LWC (Figure A.6a of the main text).

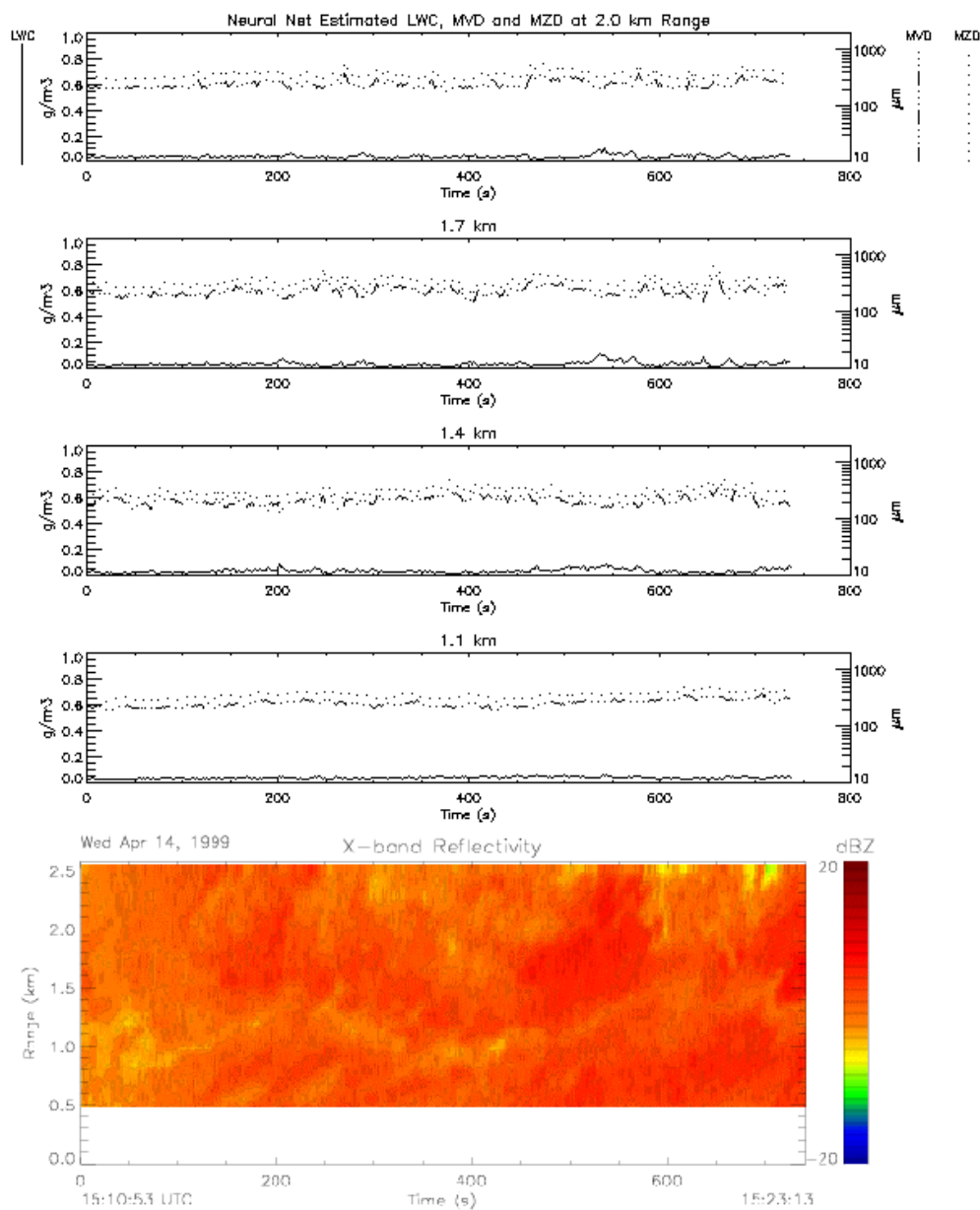


Figure A.1 Time profiles of *LWC* (solid line), *MVD* (lower dashed line) and *MZD* (upper dashed line) for April 14, 1999, 15:10 to 15:23 UTC at 1.1, 1.4, 1.7 and 2.0 km slant range. X-band reflectivity shown for reference.

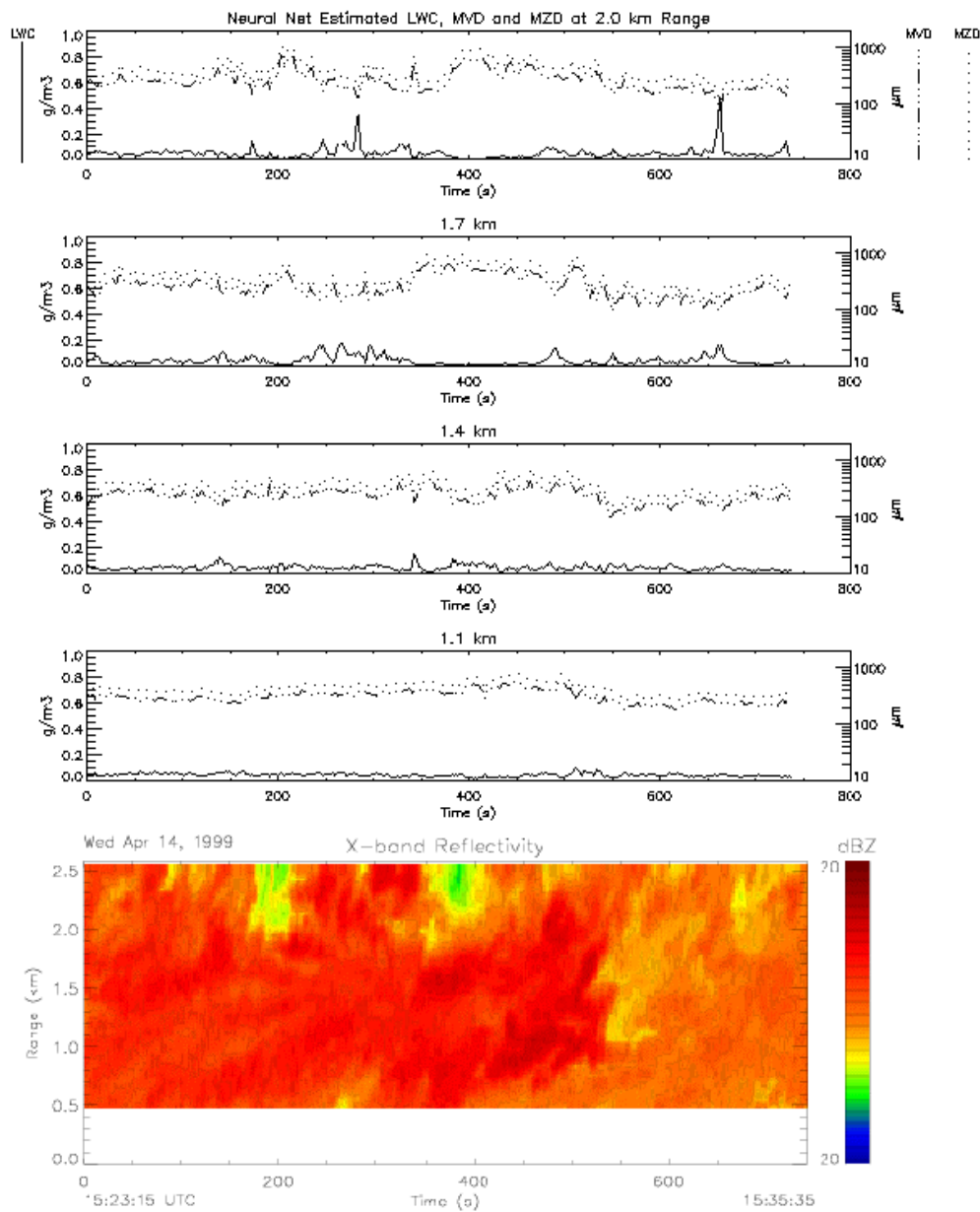


Figure A.2 Time profiles of *LWC* (solid line), *MVD* (lower dashed line) and *MZD* (upper dashed line) for April 14, 1999, 15:23 to 15:35 UTC at 1.1, 1.4, 1.7 and 2.0 km slant range. X-band reflectivity shown for reference.

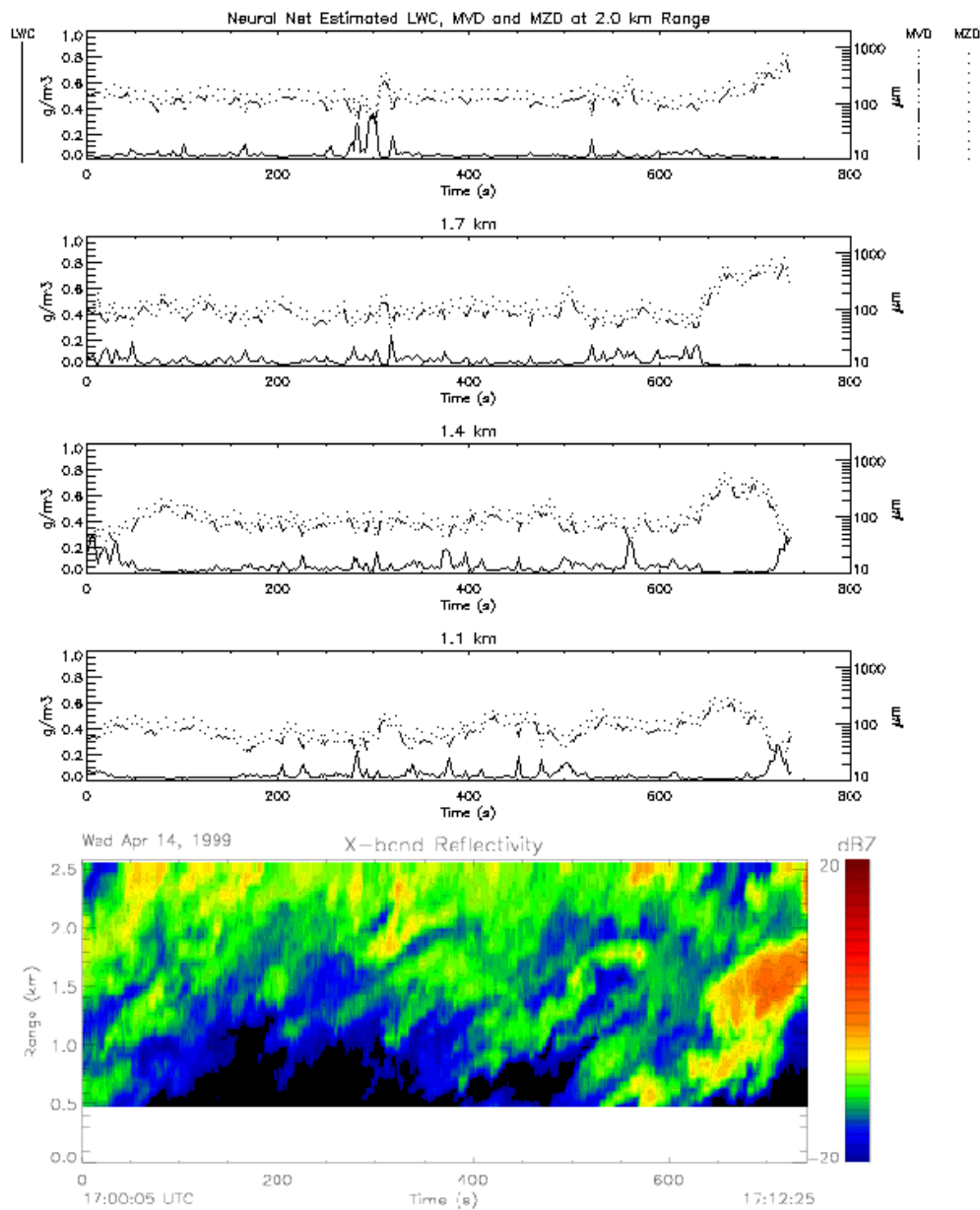


Figure A.3 Time profiles of *LWC* (solid line), *MVD* (lower dashed line) and *MZD* (upper dashed line) for April 14, 1999, 17:00 to 17:12 UTC at 1.1, 1.4, 1.7 and 2.0 km slant range.

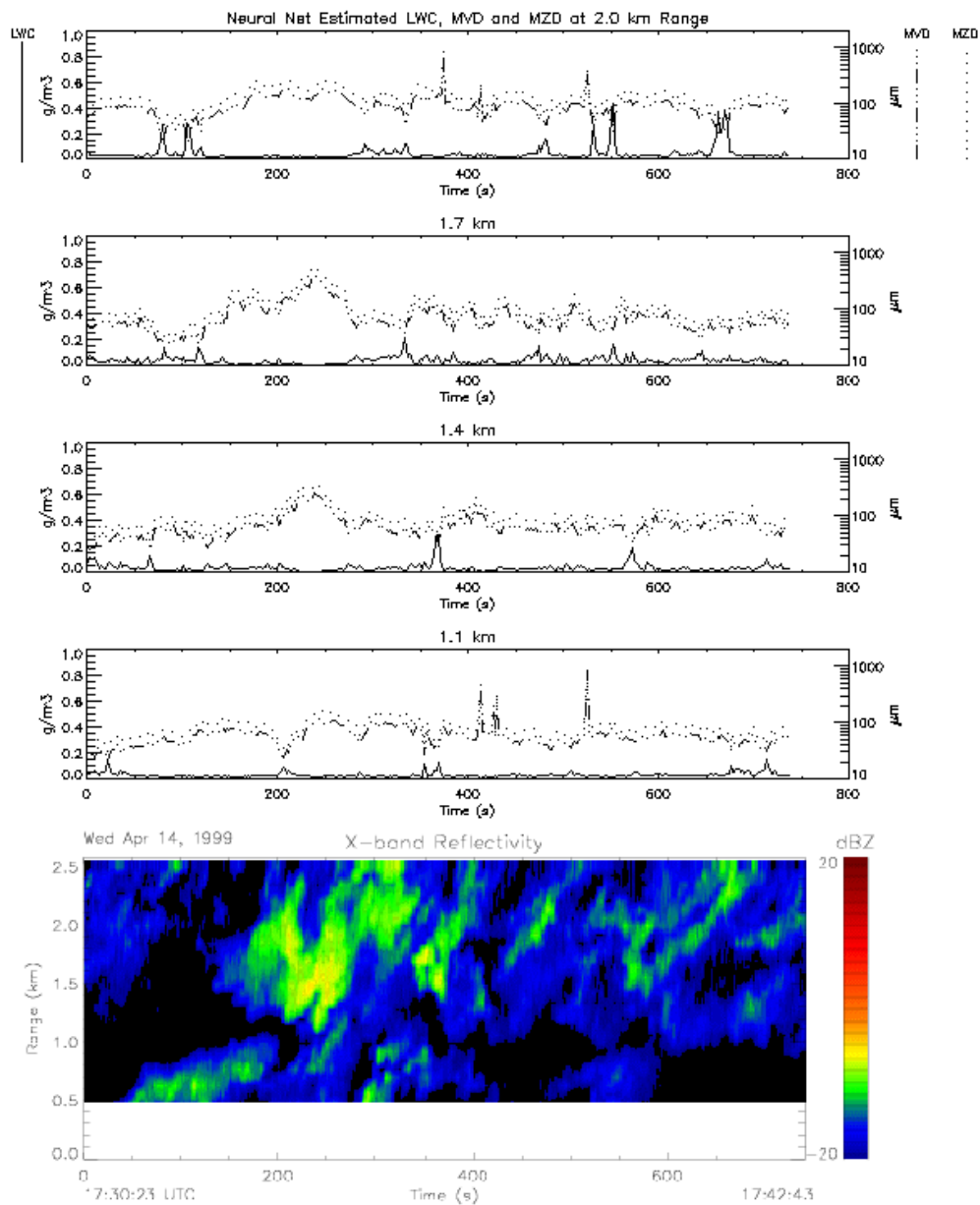


Figure A.4 Time profiles of *LWC* (solid line), *MVD* (lower dashed line) and *MZD* (upper dashed line) for April 14, 1999, 17:30 to 17:42 UTC at 1.1, 1.4, 1.7 and 2.0 km slant range.

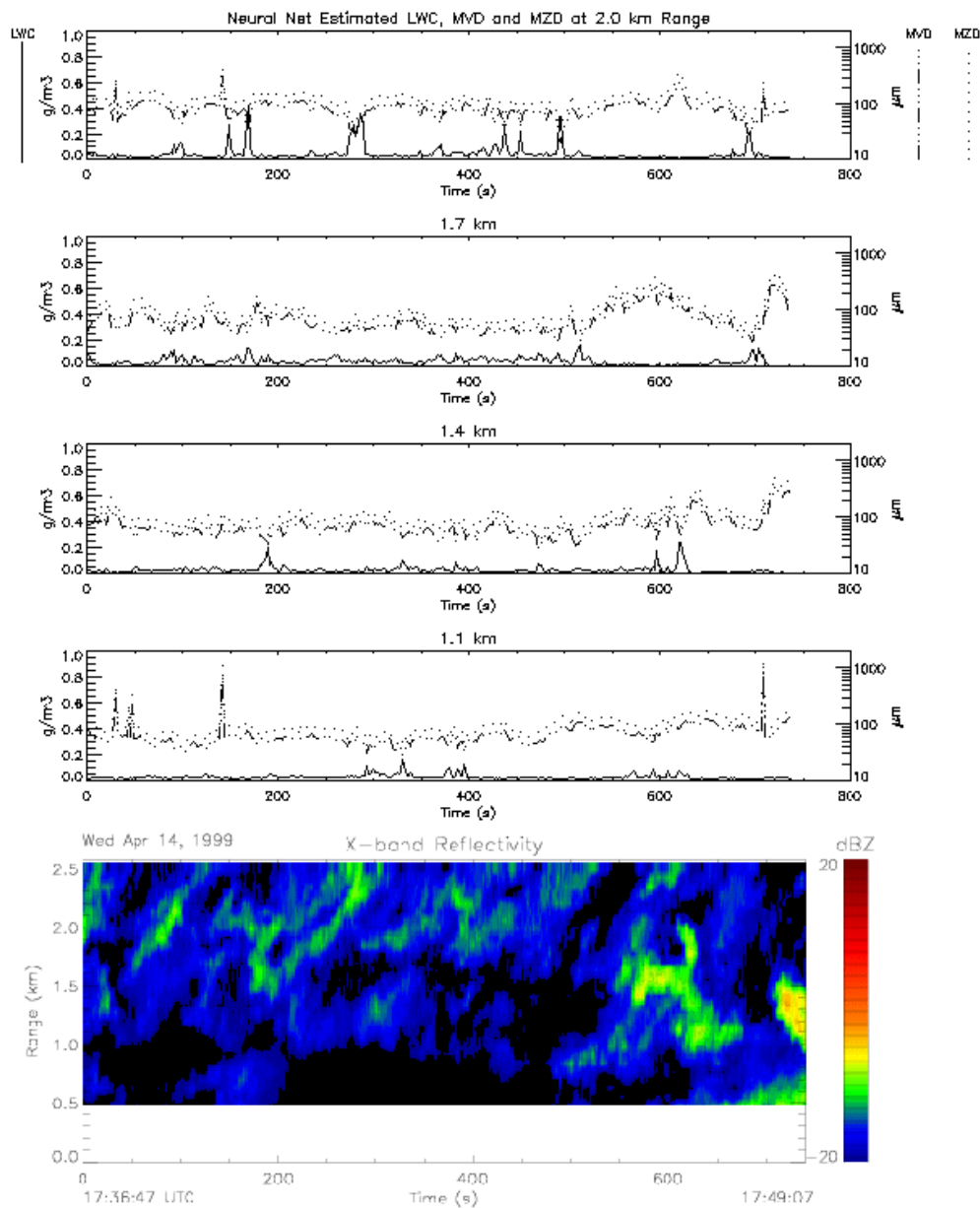


Figure A.5 Time profiles of *LWC* (solid line), *MVD* (lower dashed line) and *MZD* (upper dashed line) for April 14, 1999, 17:38 to 17:49 UTC at 1.1, 1.4, 1.7 and 2.0 km slant range.

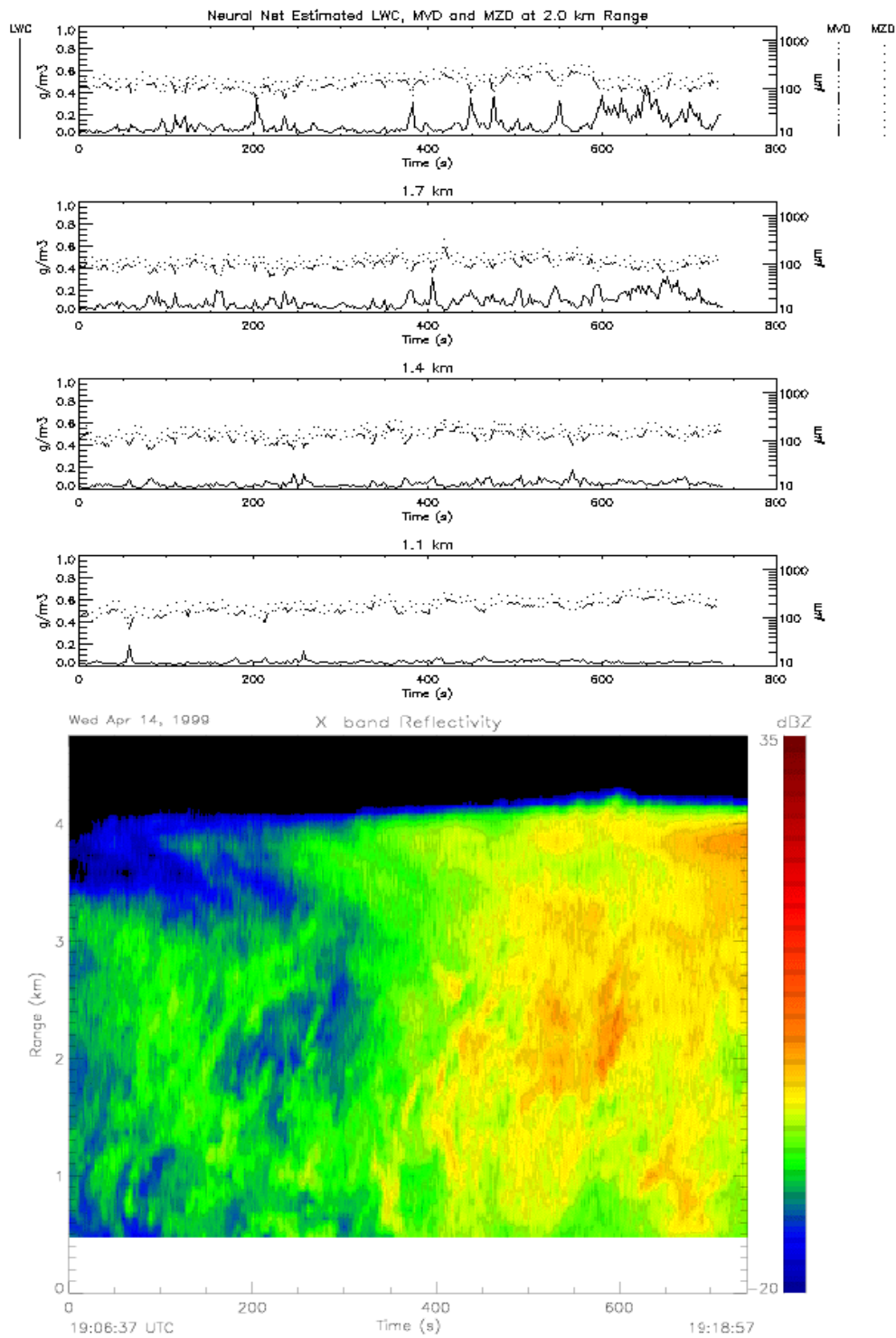


Figure A.6a Time profiles of *LWC* (solid line), *MVD* (lower dashed line) and *MZD* (upper dashed line) for April 14, 1999, 19:00 to 19:13 UTC at 1.4, 1.7, 2.0 and 2.3 km slant range.

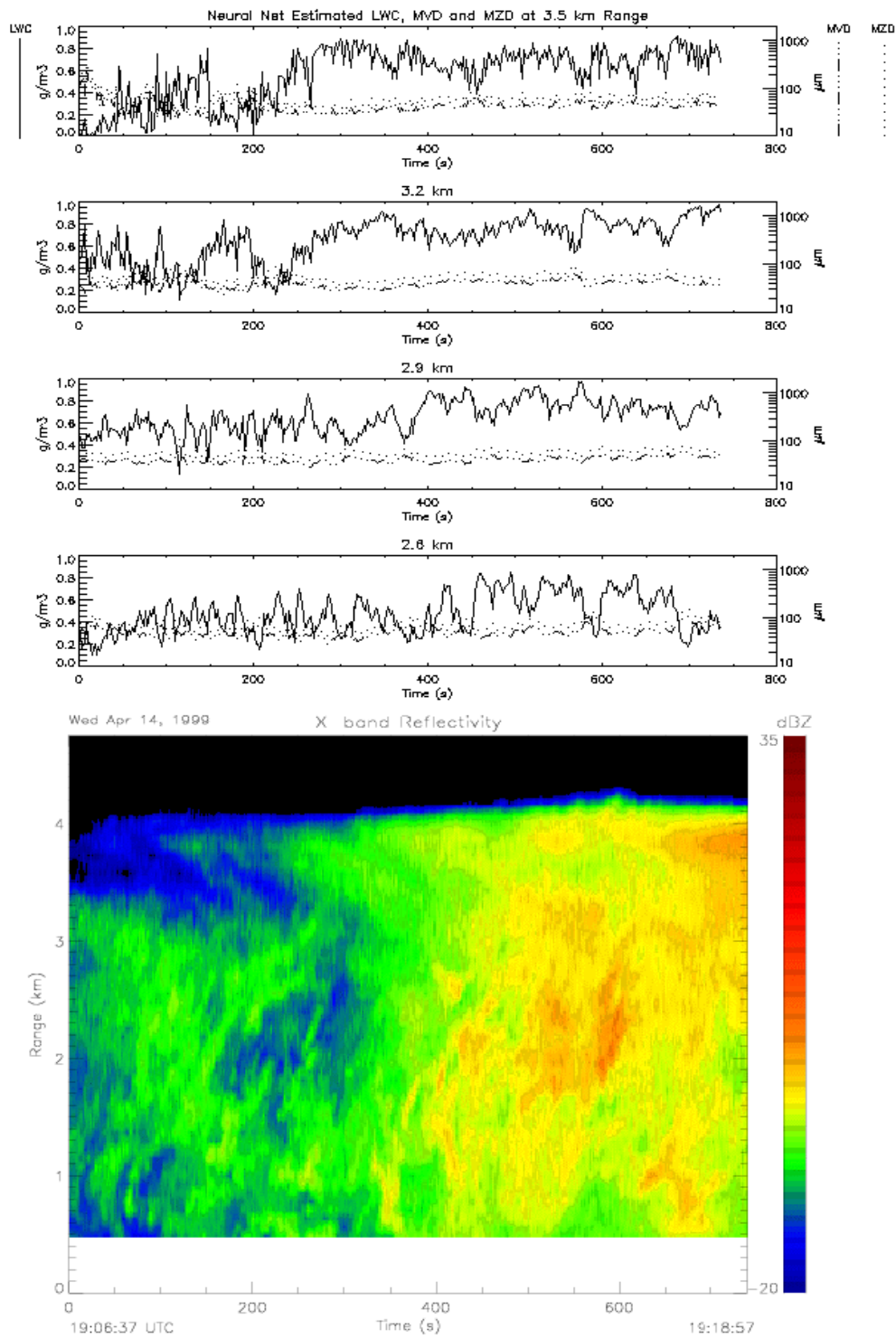


Figure A.6b Time profiles of *LWC* (solid line), *MVD* (lower dashed line) and *MZD* (upper dashed line) for April 14, 1999, 19:00 to 19:13 UTC at 2.6, 2.9, 3.2 and 3.5 km slant range.

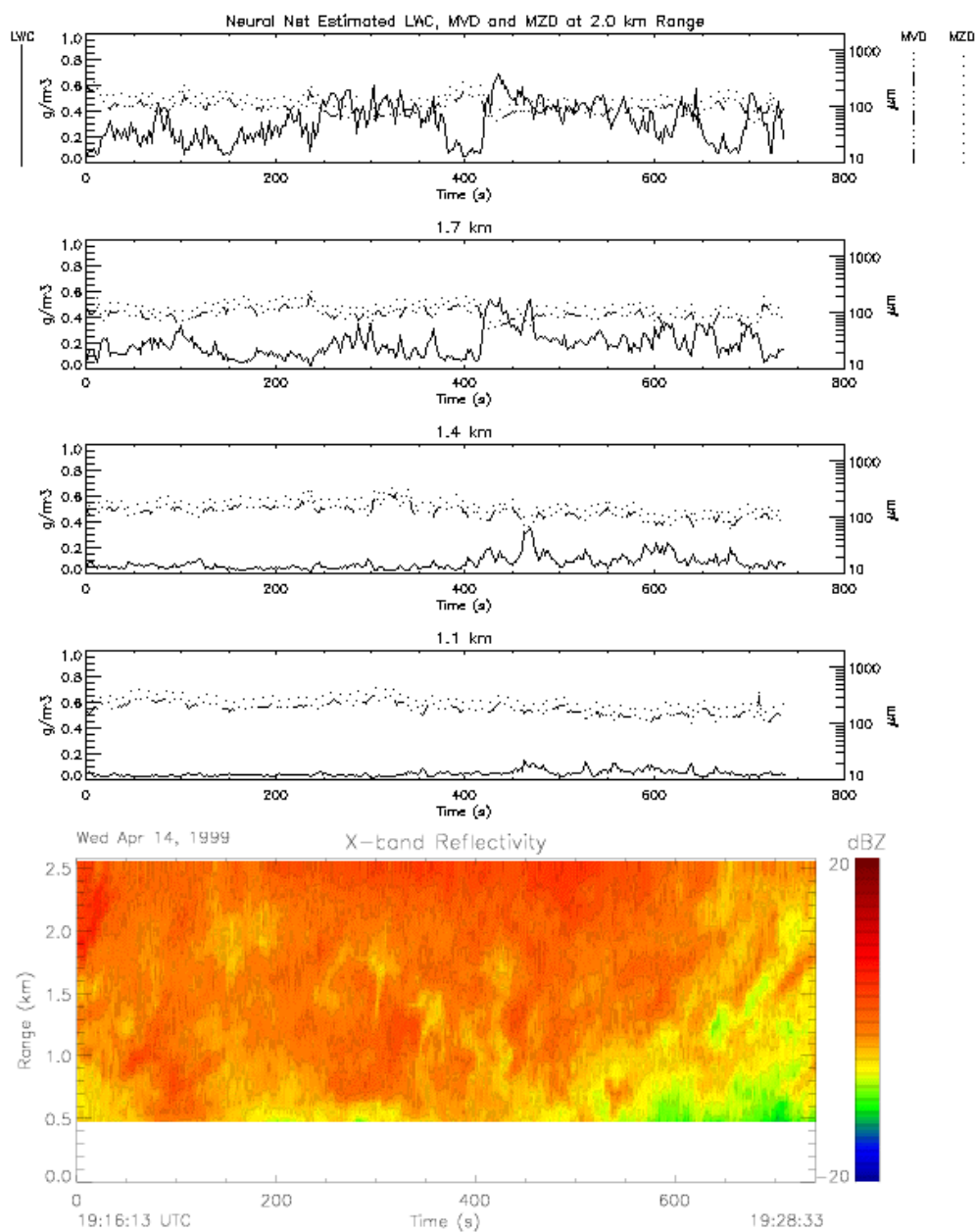


Figure A.7 Time profiles of *LWC* (solid line), *MVD* (lower dashed line) and *MZD* (upper dashed line) for April 14, 1999, 19:18 to 19:30 UTC at 1.1, 1.4, 1.7 and 2.0 km slant range.

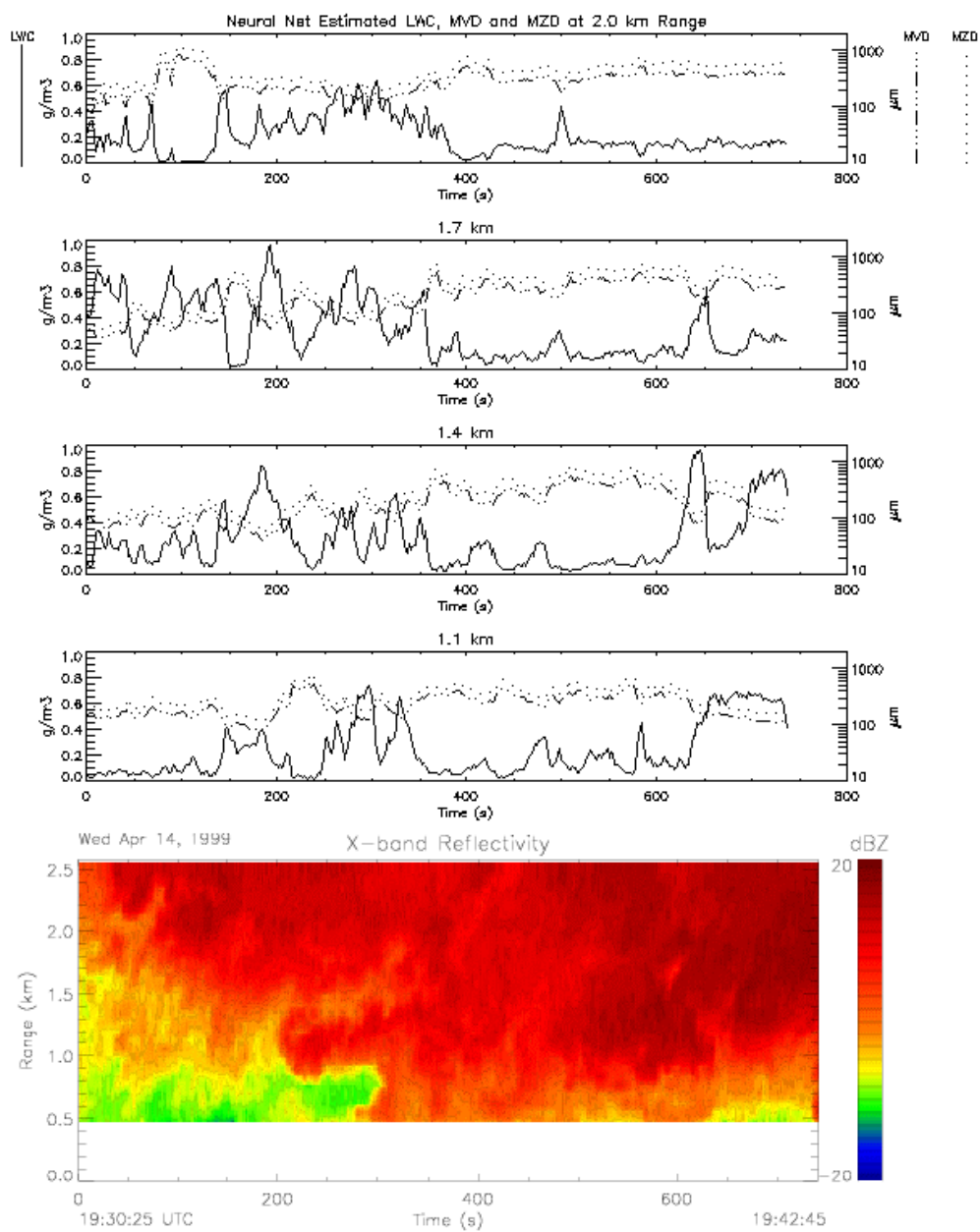


Figure A.8 Time profiles of *LWC* (solid line), *MVD* (lower dashed line) and *MZD* (upper dashed line) for April 14, 1999, 19:30 to 19:42 UTC at 1.1, 1.4, 1.7 and 2.0 km slant range.

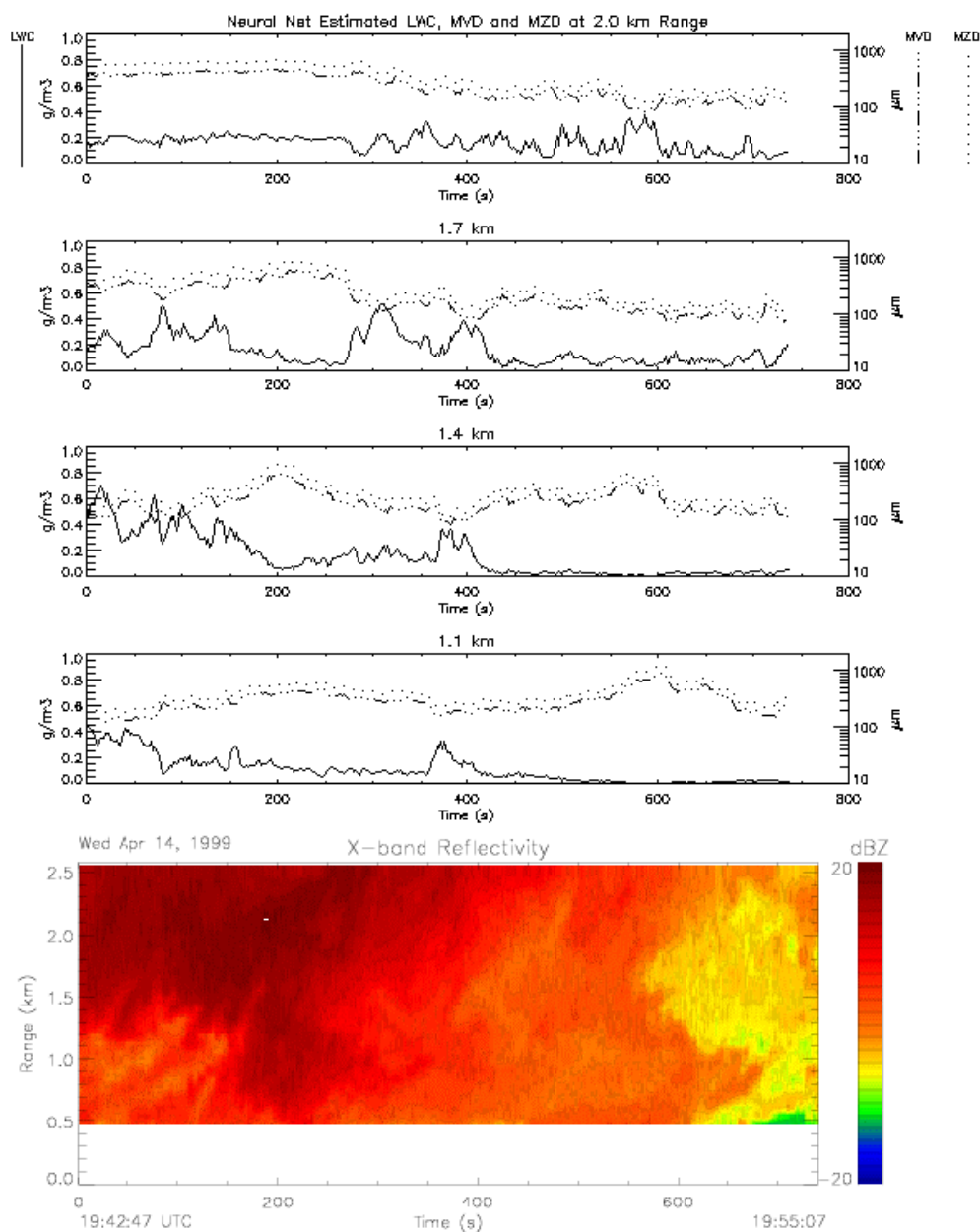


Figure A.9 Time profiles of *LWC* (solid line), *MVD* (lower dashed line) and *MZD* (upper dashed line) for April 14, 1999, 19:42 to 19:55 UTC at 1.1, 1.4, 1.7 and 2.0 km slant range.

April 15, 1999

Weather log entry:

Date: 15 april

Time: 18z

Entry by: m politovich

Entry:

A great day, well-coordinated and just about everything worked according to plan.

Had cloud from about 3500-11,1000 ft MSL, lots of ice and lots of water. Ice in the form of dendrites, mountain was seeing most around 200 microns, we down here at the crb saw snow as dendrites, up to 5 mm, first light then moderate rime. Some aggregates. Snow was showery.

Big event was the NASA Twin Otter over-flight. They made 6 passes over us from cloud top down to 8.3Kft, their minimum altitude. They saw at their lower levels lwc fairly sustained at 0.1g/m³, some values to 0.2 g/m³. Lots of dendrites, aggregates and "irregulars". It takes them 12 min to make a circuit -- coming south from north of the mountain, then turning toward the west at the crb and flying 20 miles out. Then do it again.

crb sensors all working well during the flight in "scan" mode. Lidar off, of course. summit probes also all working during the flight. Radio communication was very smooth, and we had some nice comparisons between the airborne and ground measurements.

In spite of being called a "great day", April 15, 1999 only yielded 12 minutes worth of data in coordinated observation modes between the UMass CPRS and NOAA X-band radars. The retrieved data, however, did confirm the presence of liquid up to 0.4 gm⁻³ in the farthest retrieved volume cell and the presence of large particles (ice crystals) with MZD-s up to 1 mm. This, of course, is a liquid equivalent measure of drop size, so crystal sizes were likely several times larger the cog railway base reported snow and dendrites up to 5 mm in diameter.

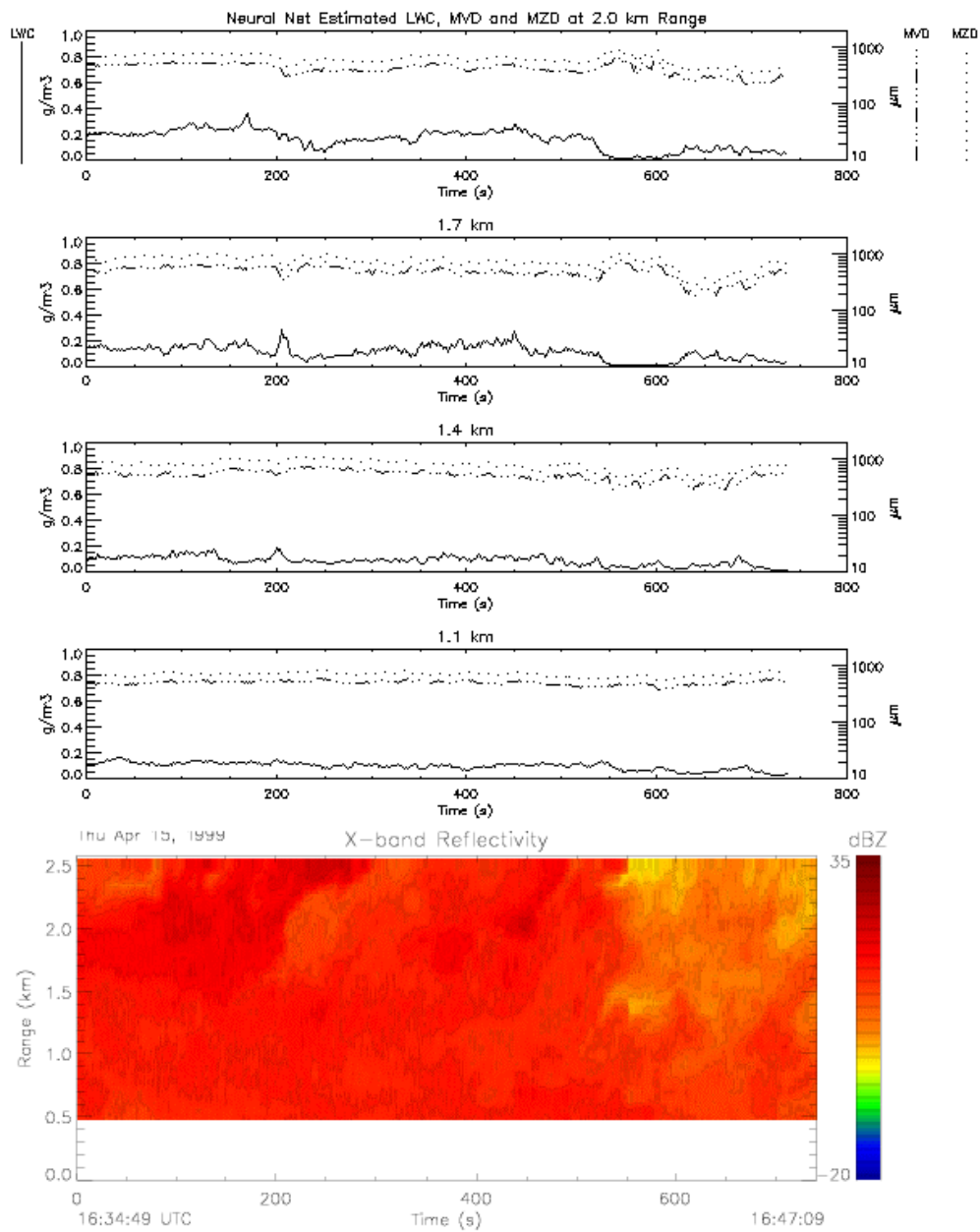


Figure A.10 Time profiles of *LWC* (solid line), *MVD* (lower dashed line) and *MZD* (upper dashed line) for April 15, 1999, 18:34 to 18:47 UTC at 1.1, 1.4, 1.7 and 2.0 km slant range.

April 17, 1999

Weather log entry:

Date: 17 april

Time: 0135z

Entry by: m politovich

Entry: Well, today was one of those days that OD's (operations directors) really dread. Weather is supposed to move in sometime in late afternoon through mid-evening. Plane can't fly after dark. Radars and summit sensors can't work too late or they won't be ready for the next day, when we'll have aircraft support. If we work late and say "sorry, can't work the next day" the aircraft may well pack up and go back to Cleveland. Yet the weather coming in looks to be quite interesting. arg. Weather finally came in about 21-22 pm. Plane more-or-less called itself down, since forecasts/progs/hopes/ were not too promising. Maybe we made a bad choice, should have held with a 21z takeoff, would have caught some interesting weather. Maybe not. At any rate, sensors at the crb and summit were up and running for the passage, from the south (finally!) of a warm front. Clouds began from aloft, lowering, some precip, we had light rain at the crb but no bright band --- at first suggestive of a "warm rain" process but later revealed to be due to the freezing level being an arm's reach of the crb. Since the OD is only 5'4" this was not immediately apparent. Anyway, extremely interesting case then of southerly flow coming over the ridge formed by Mts Washington, Franklin, Eisenhower to the south, then sinking and flowing very near the surface to our valley. Refrigeration by the snow cover on the peaks? Very stable air? I vote for a cooling effect by snow cover making the airflow denser, but maybe there is a more realistic explanation.

Radars are still working, they find this interesting. That's why we're here.

Summit saw some water, then dendrites, slightly rimed, looked to be somewhat sublimated since they were in and out of cloud.

We'll break off this soon and then us early birds will head on up to the crb and launch a CLASS sonde at 6 am, to prepare some cloud top info for a 7 am telecon with NASA. Other ops slated to begin at 8 am. Bad news is that this does not allow for a big Friday night in Bretton Woods. Good news is that Bretton Woods sees no action of Friday nights.

Date: 17 april

Time: 18z

Entry by: m politovich

Entry: Today was a different cloud, warm, with abundant liquid water and ice crystals in the form of needles and columns. A good cloud for the NOAA crew -- it filled a gap in their polarization data collection. No aircraft support since for most of the time the cloud was too low in altitude for them. In fact, they are returning to Cleveland to wait this out rather than burn up time and money sitting around in a hangar in Portland, ME. They will be available to us later this week when we hope this weather pattern changes.

The neural net retrieved LWC varied from 0.2 to 0.4 gm^{-3} in the morning files. In Figures A.11 and A.12, the estimated LWC fluctuates rapidly, which may have been caused by large, Mie scattering ice crystals modulating the reflectivity gradient. The LWC retrieved from the afternoon data, in Figures A.13a and A.13b, is somewhat smoother and, after averaging the entire 12 minutes, estimated LWC shows good agreement with the base of a liquid layer measured by the ATEK probe. The neural net estimated liquid cloud base appears several hundred meters lower than that detected by the probe, which may be due to an elevating cloud, since the radar measurements preceded the probe at the liquid base by about 10 minutes.

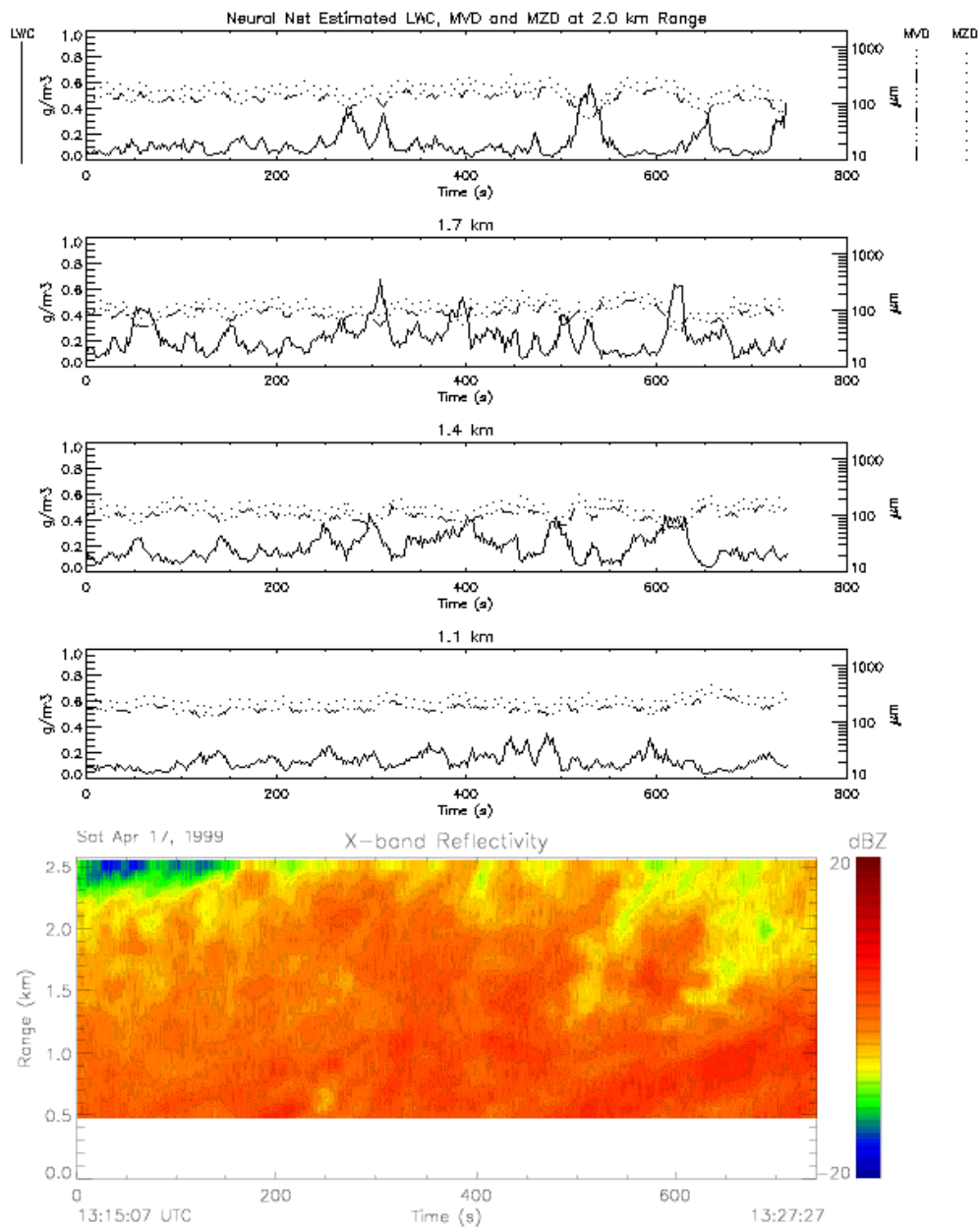


Figure A.11 Time profiles of *LWC* (solid line), *MVD* (lower dashed line) and *MZD* (upper dashed line) for April 17, 1999, 13:15 to 13:27 UTC at 1.1, 1.4, 1.7 and 2.0 km slant range.

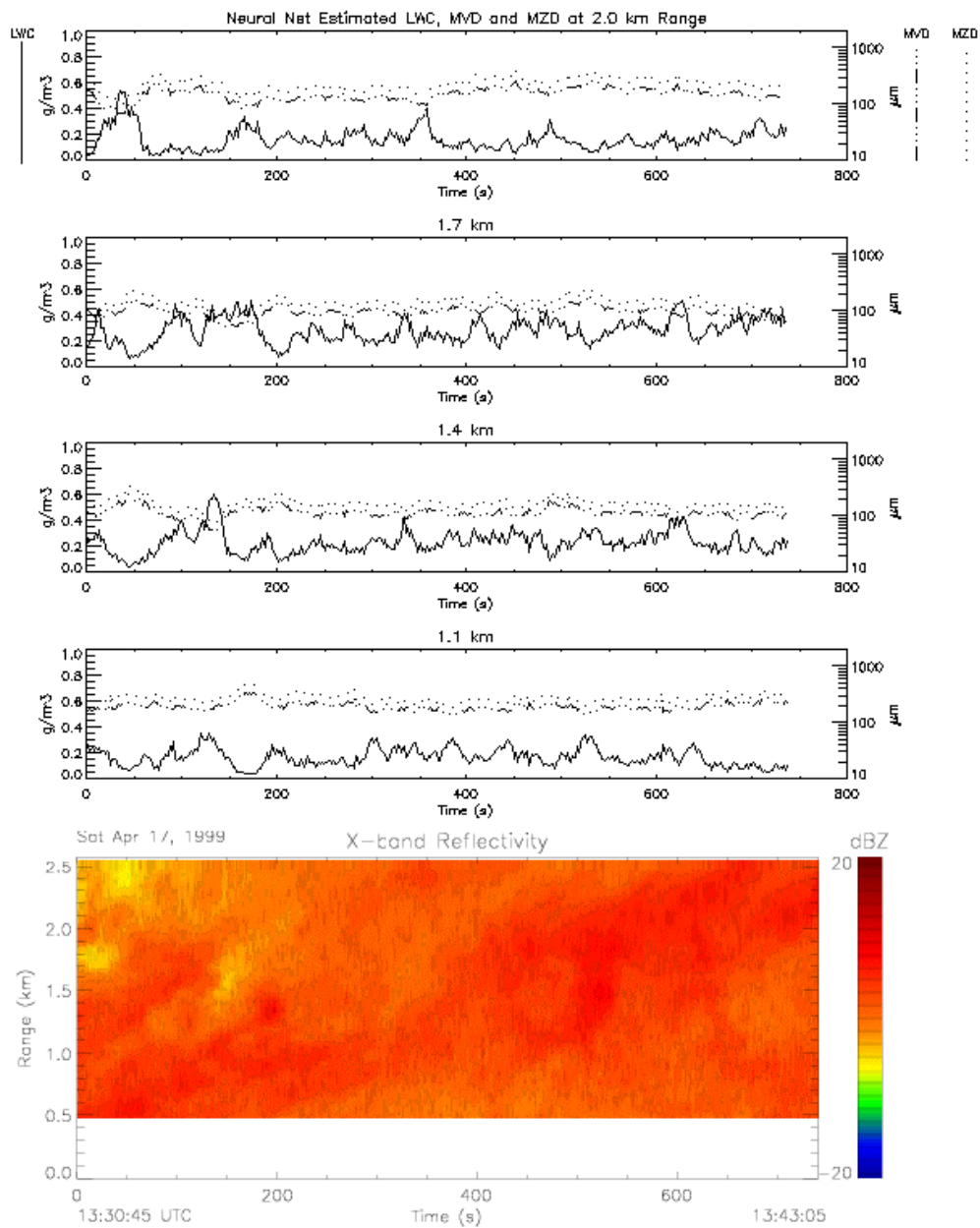


Figure A.12 Time profiles of *LWC* (solid line), *MVD* (lower dashed line) and *MZD* (upper dashed line) for April 17, 1999, 13:30 to 13:43 UTC at 1.1, 1.4, 1.7 and 2.0 km slant range.

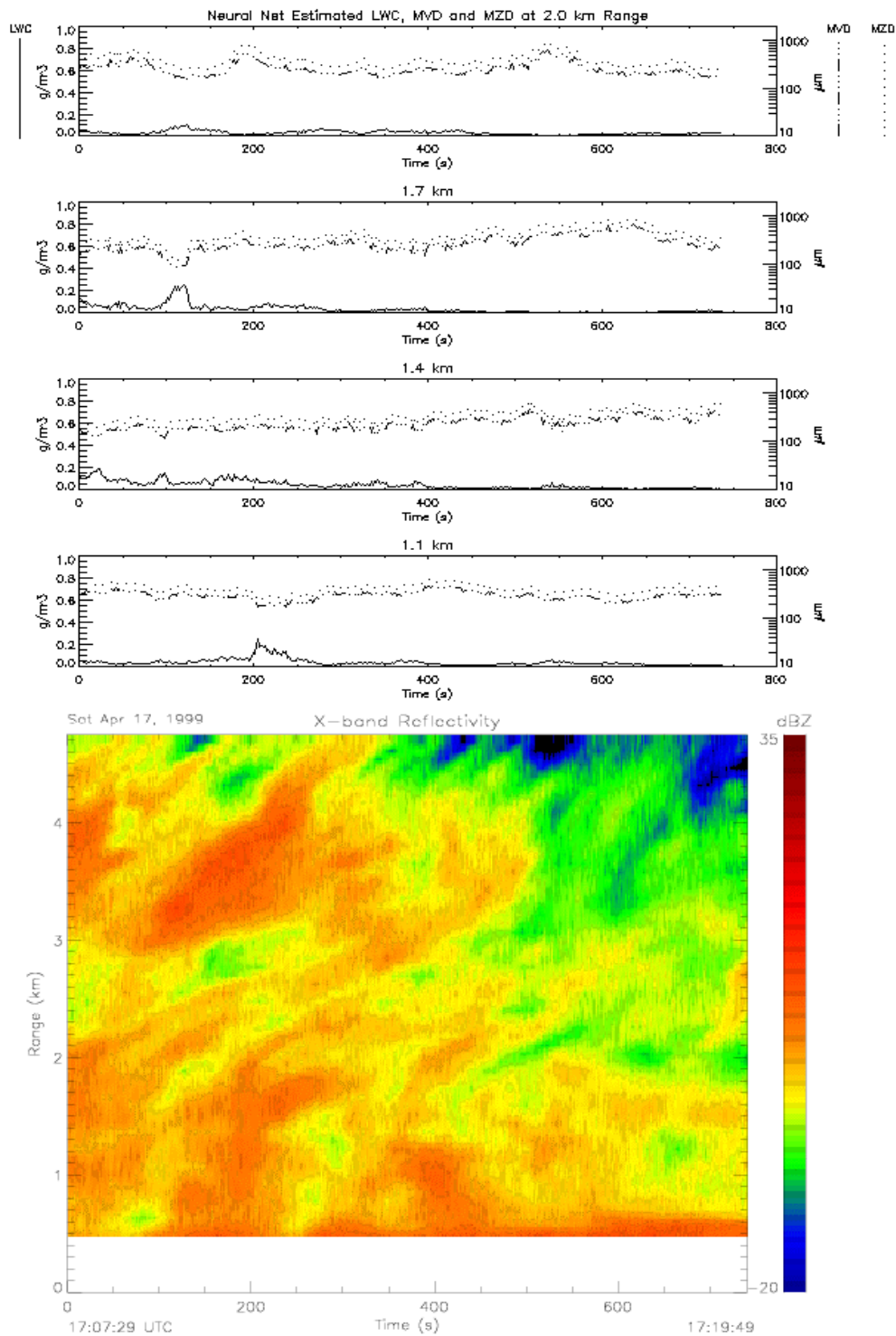


Figure A.13a Time profiles of *LWC* (solid line), *MVD* (lower dashed line) and *MZD* (upper dashed line) for April 17, 1999, 17:07 to 17:19 UTC at 1.4, 1.7, 2.0 and 2.3 km slant range.

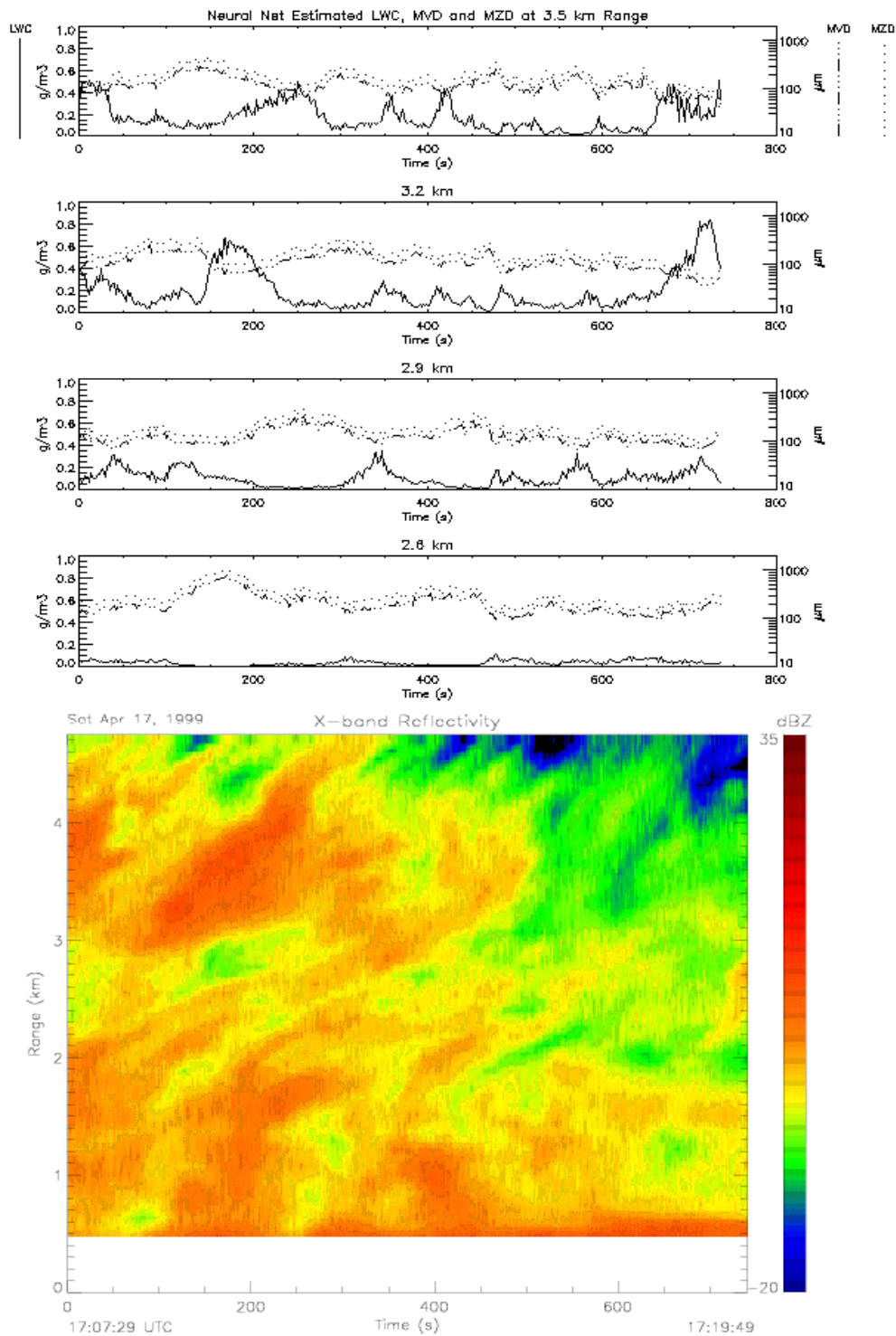


Figure A.13b Time profiles of *LWC* (solid line), *MVD* (lower dashed line) and *MZD* (upper dashed line) for April 17, 1999, 17:07 to 17:19 UTC at 2.6, 2.9, 3.2 and 3.5 km slant range.

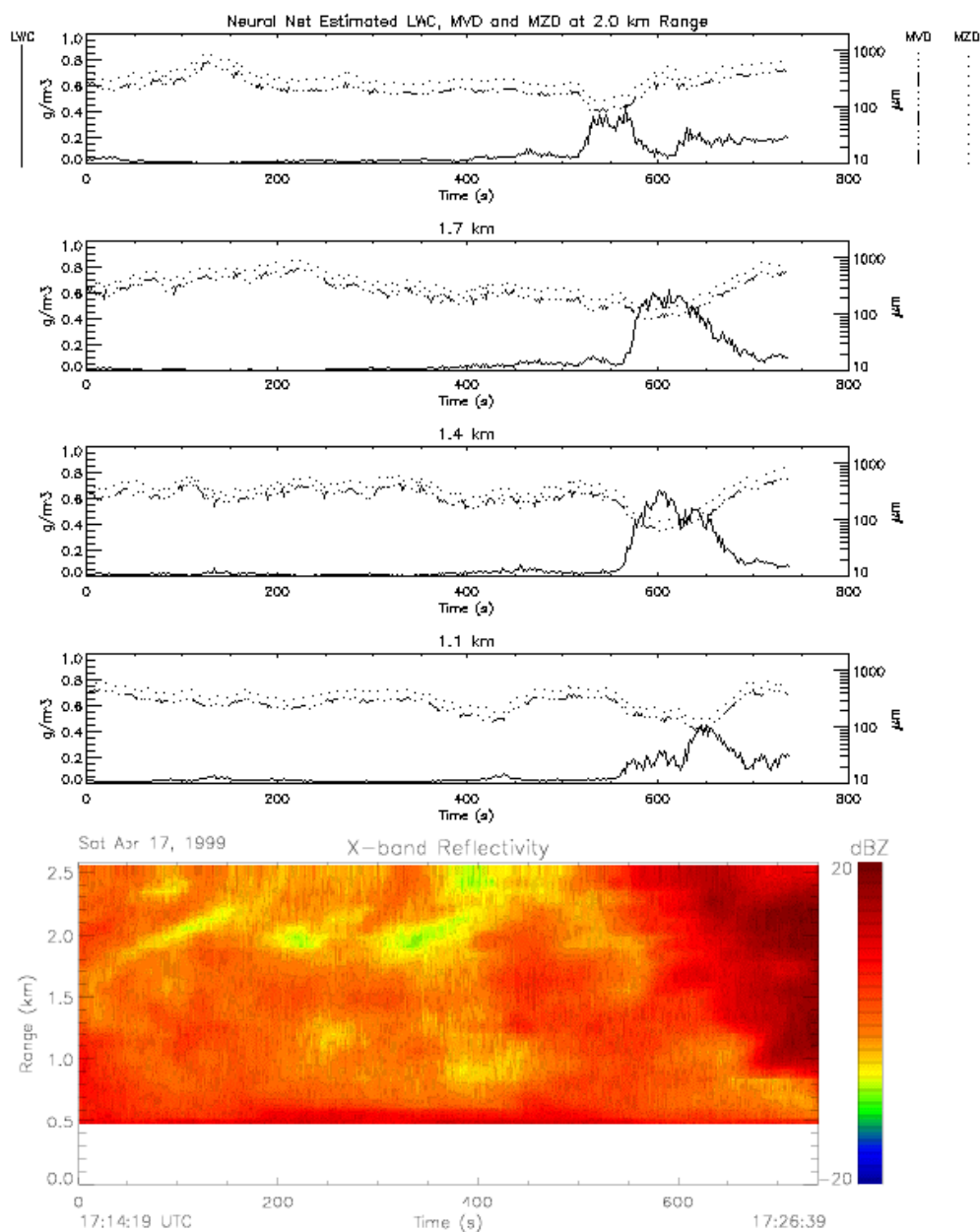


Figure A.14 Time profiles of *LWC* (solid line), *MVD* (lower dashed line) and *MZD* (upper dashed line) for April 17, 1999, 17:14 to 17:28 UTC at 1.1, 1.4, 1.7 and 2.0 km slant range.

April 20, 1999

Weather log entry:

Date: 20 april

Time: 2130z

Entry by: m politovich

Entry: A day of low winds and lots of local convection. Winds all the way up, from our rawinsonde, were well below 10 m/s -- balloon stayed pretty much in our backyard its entire flight. Had several good, heavy graupel showers which the NOAA folks appreciated for some polarization studies. Also the convective clouds were deep and contained lots of liquid, so we may be able to get some lwc retrievals out of this. The only real problems were the highly variable conditions, which "come with the territory" when you're dealing with weakly forced convection, and the fact that the observatory was only in scud at best. Moreover, the weak winds made it very difficult for their probes to sample properly.

Tomorrow looks to be similar, perhaps somewhat warmer. The whole weather pattern begins to shift north late tomorrow into Thursday, maybe putting us more in the path of whatever moisture impulses happen along --- as for now, they are just skimming to our south. We see a nice blob (for lack of a better term) of moisture entering the Great Lakes area at the present time, perhaps it's our weather feature for Friday.

The retrieved drop sizes were large, up to 1 mm consistently throughout the day's data, confirming the "heavy graupel shower" visual observations. LWC smoothly varied around 0.2 gm^{-3} with pockets of higher concentrations reaching above 0.4 gm^{-3} . Unfortunately, no in situ measurements were available on this day around the time periods of coordinated radar observations.

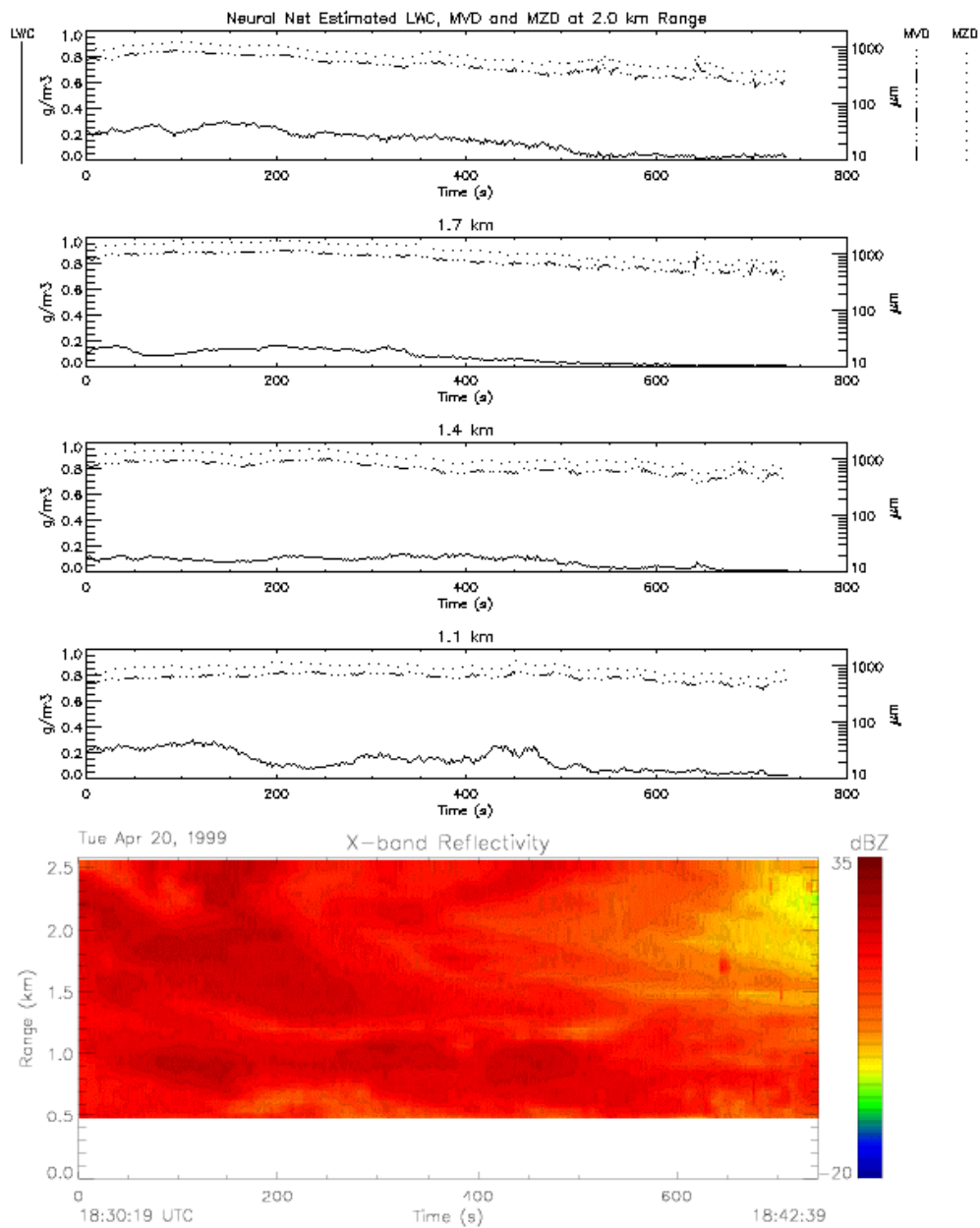


Figure A.15 Time profiles of *LWC* (solid line), *MVD* (lower dashed line) and *MZD* (upper dashed line) for April 20, 1999, 18:30 to 18:42 UTC at 1.1, 1.4, 1.7 and 2.0 km slant range.

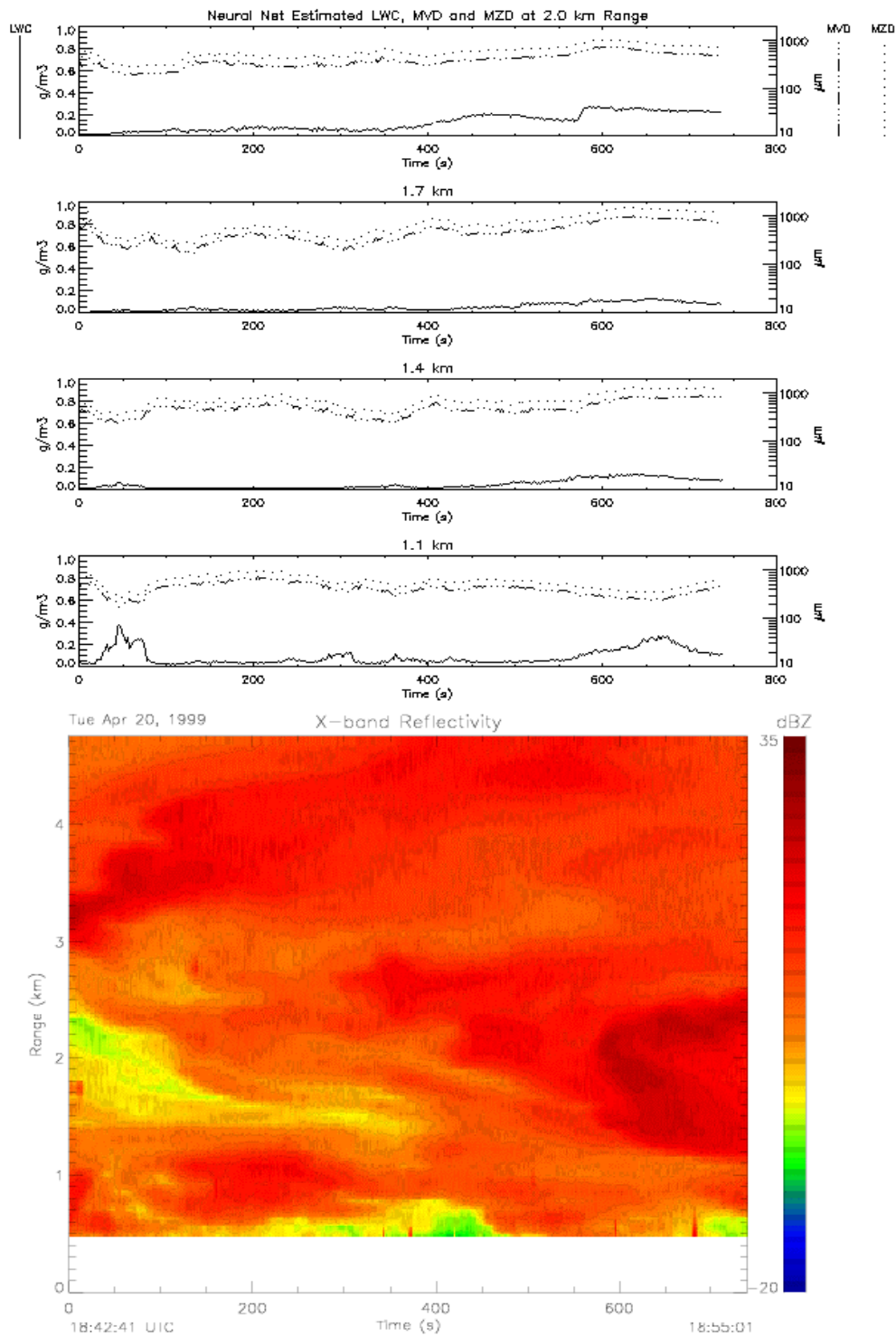


Figure A.16a Time profiles of *LWC* (solid line), *MVD* (lower dashed line) and *MZD* (upper dashed line) for April 20, 1999, 18:42 to 18:55 UTC at 1.4, 1.7, 2.0, and 2.3 km slant range.

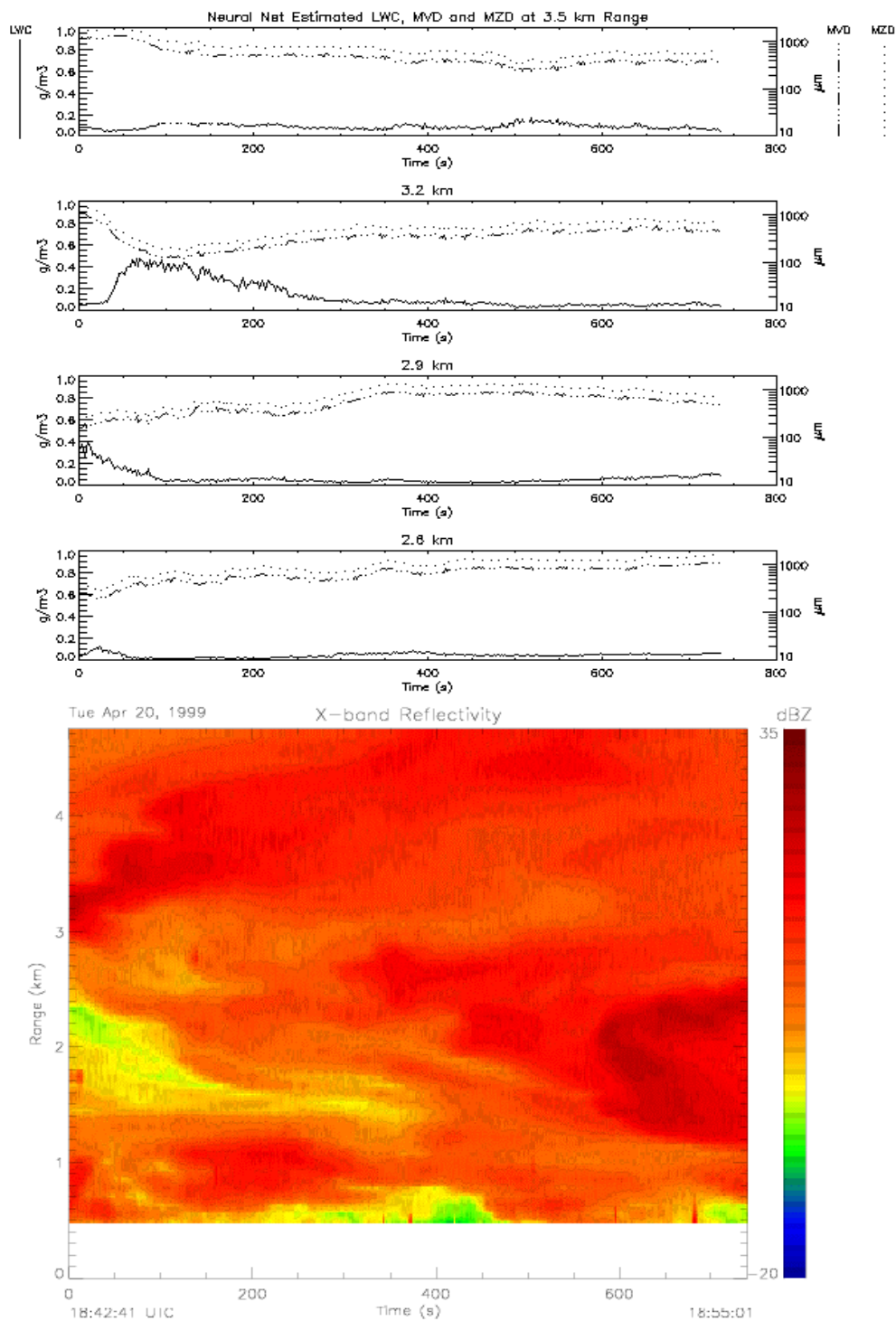


Figure A.16b Time profiles of *LWC* (solid line), *MVD* (lower dashed line) and *MZD* (upper dashed line) for April 20, 1999, 18:42 to 18:55 UTC at 2.6, 2.9, 3.2 and 3.5 km slant range.

April 26, 1999

Weather log entry:

Date: 26 april

Time: 21z

Entry by: m politovich

Entry: Busy day --- but not the weather we were led to expect. Best we could muster was some fairly decent convection. High liquid water content in the clouds but they were rather short-lived, scattered about, and in many cases, shallow.

A cold surge came through at about 1015z with a snow shower followed by brief light rain, this came during our balloon launch. At that time things looked pretty good. Then it cleared after the surge -- however we had already launched the aircraft and they unfortunately missed the action.

Just after they turned back for Portland, ME, their base of operations, local convection began popping. It started as orographically-induced light convection, then deepened and we began a series of squalls that moved through fairly methodically every half hour or so. Good graupel and rain showers, usually beginning as rain then going to graupel near the end. Some of the graupel was up to 0.5 to 0.75 cm in size, and conical. Got the aircraft into our last cell (well, now at 21z we're having one final fling with a shower passing through) where they made three passes before the storm cleared and measured liquid water contents up to 0.7g/m³.

Had lightning in the area which not only made us nervous but popped the breakers on the K-band radar and blew out the intercom in the lidar van. Observatory had a hit at one of the chimneys on top --- Marsha, the volunteer cook of the week was putting some discarded food out nearby for the ravens, and was lucky not to be injured, but did get a good scare and a tingle. Did not hear if the ravens were also affected.

The X-band radar reflectivity image and the corresponding neural net retrieved *LWC*, *MVD*, and *MZD*, shown in Figure A.17 (and Figure 5 in the main text), were collected through a melting layer at a 19 deg slant angle. Although, in situ data was not available for comparison, the melting layer qualitatively verified the results of the algorithm. The top of the bright band (melting band) is around 1.3 km slant range - just below the second of four range cells of retrieved precipitation parameters. Above the melting band *LWC* is just above 0.2 gm⁻³ and the particle size parameters are around 1.0 to 1.5 mm, indicating large ice crystals with some super-cooled liquid. The lowest range cell, centered at the bottom of the bright band, however, shows a much higher *LWC*, up to 0.8 gm⁻³, and

distinctly smaller drops ranging from 0.5 to 1 mm, confirming the melting of the ice crystals into smaller liquid hydrometeors.

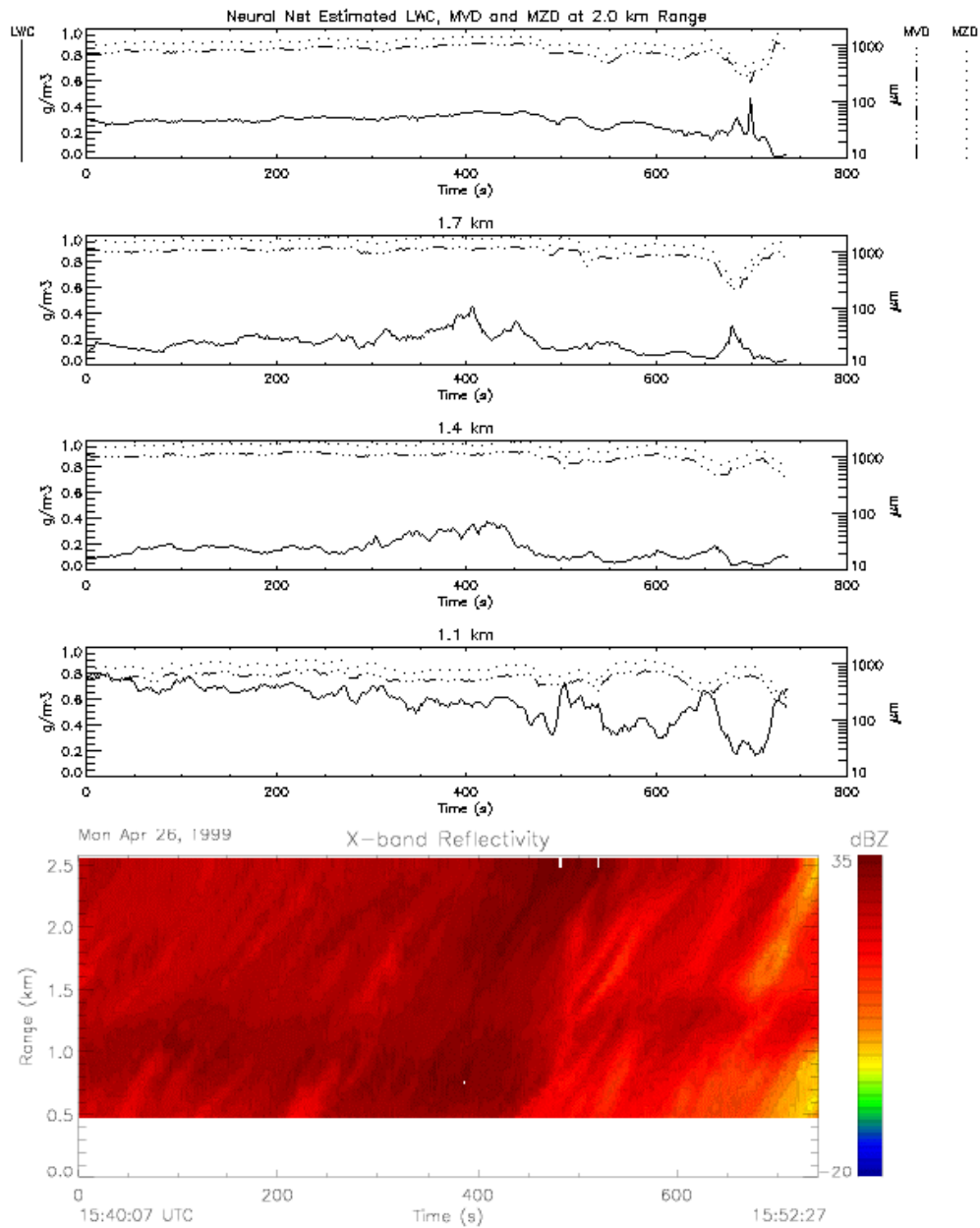


Figure A.17 Time profiles of *LWC* (solid line), *MVD* (lower dashed line) and *MZD* (upper dashed line) for April 26, 1999, 15:40 to 15:42 UTC at 1.1, 1.4, 1.7 and 2.0 km slant range.

REPORT DOCUMENTATION PAGE			Form Approved OMB No. 0704-0188	
Public reporting burden for this collection of information is estimated to average 1 hour per response, including the time for reviewing instructions, searching existing data sources, gathering and maintaining the data needed, and completing and reviewing the collection of information. Send comments regarding this burden estimate or any other aspect of this collection of information, including suggestions for reducing this burden, to Washington Headquarters Services, Directorate for Information Operations and Reports, 1215 Jefferson Davis Highway, Suite 1204, Arlington, VA 22202-4302, and to the Office of Management and Budget, Paperwork Reduction Project (0704-0188), Washington, DC 20503.				
1. AGENCY USE ONLY (Leave blank)		2. REPORT DATE August 2001		3. REPORT TYPE AND DATES COVERED Final Contractor Report
4. TITLE AND SUBTITLE Millimeter-Wave Radar Field Measurements and Inversion of Cloud Parameters for the 1999 Mt. Washington Icing Sensors Project			5. FUNDING NUMBERS WU-711-21-23-00 C-75630-J	
6. AUTHOR(S) Andrew L. Pazmany				
7. PERFORMING ORGANIZATION NAME(S) AND ADDRESS(ES) Quadrant Engineering, Inc. 107 Sunderland Road Amherst, Massachusetts 01002			8. PERFORMING ORGANIZATION REPORT NUMBER E-12948	
9. SPONSORING/MONITORING AGENCY NAME(S) AND ADDRESS(ES) National Aeronautics and Space Administration Washington, DC 20546-0001			10. SPONSORING/MONITORING AGENCY REPORT NUMBER NASA CR-2001-211103	
11. SUPPLEMENTARY NOTES Project Manager, Andrew Reehorst, Turbomachinery and Propulsion Systems Division, NASA Glenn Research Center, organization code 5840, 216-433-3938.				
12a. DISTRIBUTION/AVAILABILITY STATEMENT Unclassified - Unlimited Subject Category: 03 Available electronically at http://gltrs.grc.nasa.gov/GLTRS This publication is available from the NASA Center for AeroSpace Information, 301-621-0390.			12b. DISTRIBUTION CODE	
13. ABSTRACT (Maximum 200 words) The Mount Washington Icing Sensors Project (MWISP) was a multi-investigator experiment with participants from Quadrant Engineering, NOAA Environmental Technology Laboratory (NOAA/ETL), the Microwave Remote Sensing Laboratory (MIRSL) of the University of Massachusetts (UMass), and others. Radar systems from UMass and NOAA/ETL were used to measure X-, Ka-, and W-band backscatter data from the base of Mt. Washington, while simultaneous in-situ particle measurements were made from aircraft and from the observatory at the summit. This report presents range and time profiles of liquid water content and particle size parameters derived from range profiles of radar reflectivity as measured at X-, Ka-, and W-band (9.3, 33.1, and 94.9 GHz) using an artificial neural network inversion algorithm. In this report, we provide a brief description of the experiment configuration, radar systems, and a review of the artificial neural network used to extract cloud parameters from the radar data. Time histories of liquid water content (LWC), mean volume diameter (MVD) and mean Z diameter (MZD) are plotted at 300 m range intervals for slant ranges between 1.1 and 4 km. Appendix A provides details on the extraction of radar reflectivity from measured radar power, and Appendix B provides summary logs of the weather conditions for each day in which we processed data.				
14. SUBJECT TERMS Aircraft icing; Drop size; Liquid water content; Operations; Radar; Remote sensing			15. NUMBER OF PAGES 48	
			16. PRICE CODE	
17. SECURITY CLASSIFICATION OF REPORT Unclassified	18. SECURITY CLASSIFICATION OF THIS PAGE Unclassified	19. SECURITY CLASSIFICATION OF ABSTRACT Unclassified	20. LIMITATION OF ABSTRACT	